**Uncharacterized yeast gene *YBR238C*, an effector of TORC1 signaling in a mitochondrial feedback loop, accelerates cellular aging via *HAP4*- and *RMD9*-dependent mechanisms**

Mohammad Alfatah[1*], Jolyn Lim Jia Jia[1#], Yizhong Zhang[1#], Arshia Naaz[2#], Trishia Yi Ning Cheng[1#], Sonia Yogasundaram[1], Nashrul Afiq Faidzinn[1], Jovian Lin Jing[1], Birgit Eisenhaber[1,2,3], and Frank Eisenhaber[1,2,3,4]

Affiliations:

1. Bioinformatics Institute (BII), Agency for Science, Technology and Research (A*STAR), 30 Biopolis Street, Matrix #07-01, Singapore 138671, Republic of Singapore
2. Genome Institute of Singapore (GIS), Agency for Science, Technology and Research (A*STAR), 60 Biopolis Street, Genome #02-01, Singapore 138672, Republic of Singapore
3. LASA – Lausitz Advanced Scientific Applications gGmbH, Straße der Einheit 2-24, D-02943 Weißwasser, Federal Republic of Germany
4. School of Biological Sciences (SBS), Nanyang Technological University (NTU), 60 Nanyang Drive, Singapore 637551, Republic of Singapore

#Equal authorship contributions

*To whom the correspondence should be addressed.
Email: alfatahm@bii.a-star.edu.sg (Mohammad Alfatah)

**SUMMARY**

Uncovering the regulators of cellular aging will unravel the complexity of aging biology and identify potential therapeutic interventions to delay the onset and progress of chronic, aging-related diseases. In this work, we systematically compared gene sets involved in regulating the lifespan of *Saccharomyces cerevisiae* (a powerful model organism to study the cellular aging of humans) and those with expression changes under rapamycin treatment. Among the functionally uncharacterized genes in the overlap set, *YBR238C* stood out as the only one downregulated by rapamycin and with an increased chronological and replicative lifespan upon deletion. We show that *YBR238C* and its paralogue *RMD9* oppositely affect mitochondria and aging. *YBR238C* deletion increases the cellular lifespan by enhancing mitochondrial function. Its overexpression accelerates cellular aging via mitochondrial dysfunction. We find that the phenotypic effect of *YBR238C* is largely explained by *HAP4*- and *RMD9*-dependent mechanisms. Further, we find that genetic or chemical-based induction of mitochondrial dysfunction increases TORC1 (Target of Rapamycin Complex 1) activity that, subsequently, accelerates cellular aging. Notably, TORC1 inhibition by rapamycin (or deletion of *YBR238C*) improves the shortened lifespan under these mitochondrial dysfunction conditions in yeast and human cells. The growth of mutant cells (a proxy of TORC1 activity) with enhanced mitochondrial function is sensitive to rapamycin whereas the growth of defective mitochondrial mutants is largely resistant to rapamycin compared to wild type. Our findings demonstrate a feedback loop between TORC1 and mitochondria (the TORC1-MItochondria-TORC1 (TOMITO) signaling process) that regulates cellular aging processes. Hereby, *YBR238C* is an effector of TORC1 modulating mitochondrial function.

**Keywords**

cellular aging; lifespan; nutrient signaling**;** target of rapamycin complex 1; mitochondria; uncharacterized genes; yeast; human cells

## INTRODUCTION

Healthy aging is crucially determined by cellular functions, and their defective status is associated with premature dysfunction and/or depletion of critical cell populations and various aging-associated pathologies such as neurodegenerative diseases, cancer, cardiovascular disorders, diabetes, sarcopenia and maculopathy [1–6]. Advancements in biomedical research including genome-wide screening in different aging model organisms, identified several biological pathways that support the unprecedented progress in understanding overlapping profiles between aged cells and different chronic aging-associated diseases [7–10]. In principle, uncovering the molecular mechanisms that drive cellular aging identifies potential drug targets and can fuel the development of therapeutics to delay aging and increase healthspan [11–14].

Given the evolutionary conservation of many aging-related pathways, yeast is one of the aging model organisms that have been extensively used to study the biology of human cellular aging by analyzing chronological lifespan (CLS) and replicative lifespan (RLS) under various conditions [15–18]. The CLS is the duration of time that a non-dividing cell is viable. This is a cellular aging model for post-mitotic human cells such as neurons and muscle cells. The RLS defines as the number of times a mother cell divides to form daughter cells. Such experiments provide a replicative human aging model for mitotic cells such as stem cells. Genome-wide or individual gene deletion strains' screening identified thousands of genes affecting cellular lifespan. These lists are a rich resource to identify unique genetic regulators, functional networks, and interactions of aging hallmarks relevant to cellular lifespan [1,4,7,11–14].

We systematically examined the available genetic data on aging and lifespan for budding yeast, *Saccharomyces cerevisiae*, from various sources. Our bioinformatics analyses revealed consensus lists of genes regulating yeast CLS and RLS. These gene sets were compared with lists of genes the expression of which changed under TORC1 inhibition with rapamycin. When we turned our attention to the functionally uncharacterized genes involved, we found *YBR238C* the only one among the latter that increases both CLS and RLS upon deletion and that is downregulated by rapamycin. Transcriptomics and biochemical experiments revealed that *YBR238C* negatively regulates mitochondrial function, largely via *HAP4*- and *RMD9*-dependent mechanisms, and thereby affects cellular lifespan. Surprisingly, *YBR238C* and its paralogue *RMD9* oppositely influence mitochondrial function and cellular aging.

Our chemical genetics and metabolic analyses unravel a feedback loop of the interaction of TORC1 with mitochondria that affect cellular aging. *YBR238C* is an effector of TORC1 that modulates mitochondrial function. We also show that mitochondrial dysfunction induces TORC1 activity enhancing cellular aging. In turn, TORC1 inhibition in yeast and human cells with mitochondrial dysfunction suppresses their accelerated cellular aging.

## RESULTS

### Genome-wide survey of genes affecting cellular lifespan in yeast in accordance with literature and public databases

Lists of scientific literature instances mentioning a yeast gene as affecting lifespan were downloaded from the databases SGD (*Saccharomyces cerevisiae* genome database) [19], and GenAge [20]. In most cases, the experiments referred to are gene deletion phenotype studies. After processing the files for the mentioning of 'increase/decrease' of 'chronological lifespan' (CLS) and/or 'replicative lifespan' (RLS) as well as the suppression of gene duplicates, we found 2399 entries with distinct yeast genes in 15 categories reported to increase/decrease CLS and/or RLS under various conditions (Table 1). We collectively call them Aging Associated Genes (AAGs). Notably, about one-third of the total yeast genome belongs to that category. Downloaded files (as of 8$^{th}$ November 2022), description of the processing details, and all the resulting gene lists are available in 'Additional File 1'.

Whereas most of the genes (1610, 67%) have been mentioned for just one of the four scenarios ("CLS increase", "CLS decrease", "RLS increase", and "RLS decrease"), the remaining genes have been described for several alternative and/or even opposite/conflicting outcomes. 19 genes are brought up in context with all four scenarios. As the experimental conditions varied among the reports and the gene networks are complex, this is not necessarily a contradiction. Yet (see below) some of the cases are actually annotation errors at the database level.

We explored the potential enrichment of gene ontology (GO) terms among the genes involved in the 15 categories with the help of DAVID WWW server [21]. The most significant result is the enrichment of ontology terms related to mitochondrial function among the genes annotated with the single qualifier "CLS decrease". The top mitochondrial term cluster has an enrichment score 18.2 (gene-wise P-values and Benjamini-Hochberg values all below 6.e-13); a second one related to mitochondrial translation has the score 4.7. Enrichment of mitochondrial

ontology terms has also been observed for "CLS decrease" in combination with "CLS increase" or "RLS increase/decrease".

Every other signal from the ontology is much weaker. Term enrichment (with scores near 2 or better) related to autophagy and vesicular transport pop up for CLS-annotated genes whereas terms connected with translation, DNA repairs, telomeres, protein degradation and signaling are observed with RLS-tagged gene lists.

We also explored the presence of uncharacterized or severely under-characterized genes in the 15 categories of AAGs (Table 1). In total, 944 genes are annotated in SGD as coding for a protein of unknown function. Additionally, we considered genes without dedicated gene name (only with six-letter locus tag) as dramatically under-characterized. Comparison of this combined list with those in the 15 categories reveals 88 severely understudied AAGs that are candidates for enhanced attention from the scientific community. Thus, functionally insufficiently characterized genes have a great role in cellular aging-related processes.

**Rapamycin response genes overlap with the AAGs**

Nutrient sensing dysregulation is one of the aging hallmarks [11,12]. The conserved protein complex Target of Rapamycin Complex 1 (TORC1) senses nutrients such as amino acids and glucose and links metabolism with cellular growth and proliferation [22–25]. TORC1 positively regulates aging, and its inhibition increases lifespan in various eukaryotic organisms including yeast and mammalian [13,23,24,26,27]. The drug rapamycin, initially discovered as an antifungal natural product produced by *Streptomyces hygroscopicus*, inhibits TORC1 and increases lifespan (Figures S1A and S1B) [13,17,19,21,23,25,29].

To explore the connection between nutrient signaling and cellular aging we mapped the TORC1 regulated genes with AAGs. We first identified rapamycin response genes (RRGs) by transcriptomics analysis (RNA-Seq for yeast *S. cerevisiae* BY4743 cells treated with rapamycin and DMSO control; Figure S1C). Relevant measurement results, lists of 2365 RRGs and supplementary methodical comments are available in 'Additional File 2'.

As overlap of two RNA-Seq data analysis methods (see Methods), we identified 1155 rapamycin upregulate genes (RUG) and 1210 rapamycin downregulated genes (RDG) (Figures S1D-S1F; Additional File 2). RNA-Seq results were confirmed for some genes by qRT-PCR

(Figure S2A). We also checked the differential gene expressions in prototrophic yeast *S. cerevisiae* strain CEN.PK and found similar results as with the BY4743 strain (Figure S2B). To note, our transcriptomics analyses are, as a trend, consistent with previous RNA-Seq studies carried out under partially different experimental conditions [34,35].

We mapped the RRGs (RUG and RDG) with AAGs. Among the 2399 AAGs names, 397 and 433 (in total 830) re-occur in the lists of RUG and RDG, respectively. Thus, the overlap with AAGs is nearly 35%. I.e., TORC1 controls about one third of the AAGs. Table 1 shows how many AAGs are up- and down-regulated by rapamycin treatment for each of the 15 categories with regard to CLS/RLS increase/decrease. Notably, the order of magnitude for the respective numbers of RUG and RDG is the same for all 15 studied subgroups.

Since rapamycin increases the lifespan by an inhibitory effect on TORC1 activity [13,17,19,21,23,25,29], it appears most interesting to focus on AAGs with a deletion phenotype of increased CLS/RLS and being down-regulated by rapamycin application. A manual analysis of these gene lists reveals that, among the uncharacterized or severely understudied AAGs, there is a single one known to increase both CLS and RLS upon deletion and being downregulated by rapamycin treatment. This gene is *YBR238C*.

**Uncharacterized genes mapping unravels the role of *YBR238C* in cellular aging**

Not much is known about *YBR238C* besides its effect on lifespan (to increase CLS and RLS), its mitochondrial localization [36], its transcriptional up-regulation by TORC1 and the existence of the paralogue *RMD9*. The encoded protein has 731 amino acid residues. Sequence architecture analysis with the ANNOTATOR [37] reveals an intrinsically unstructured region over the first ca. 130 residues (first, a long polar but uncharged run followed by a histidine/asparagine-rich region beginning with position 83) and a pentatricopetide repeat region (residues 130-675, for example, due to a HHpred [38] hit to structure 7A9X chain A with E-value 2.e-56). Given the sequence homology, we hypothesize that the protein encoded by *YBR238C* is involved in RNA binding as its paralogue *RMD9* with a similar globular segment [39].

To note, *YBR238C* carries the conflicting annotations in SGD for increased and decreased RLS upon deletion. Unfortunately, there is not a single direct report about *YBR238C* listed in the scientific literature at the time of writing. There are a few genome-wide deletion strain studies

that identified *YBR238C* as one of the gene that increases CLS [40] and RLS [8,41–43]. However, the SGD database wrongly documented one of the latter studies as evidence for a decreased RLS phenotype of *YBR238C* [43]. Thus, this examination allows us to claim *YBR238C* as the only uncharacterized rapamycin downregulated gene causing CLS and RLS increase upon deletion.

First, we confirmed that *YBR238C* is indeed a rapamycin response gene by qRT-PCR expression analysis in both yeast backgrounds BY4743 and CEN.PK (Figures 1A and 1B). Further, we tested the role of *YBR238C* in cellular aging by measuring the CLS in yeast. CLS was analysed in BY4743 and CEN.PK strains using three different outgrowth survival methods (see detail in methods section). Cell survival of wild type and *ybr238c*Δ strains was analysed at various age time points. We found higher CLS of *ybr238c*Δ cells compared to wild type cells (Figures 1C-1F). Together, these results confirmed that rapamycin inhibits the expression of *YBR238C*, and deletion of this gene indeed increases the cellular lifespan.

**Transcriptomics analysis reveals the longevity gene expression signatures of *ybr238c*Δ mutants**

The transcriptome of the long-lived *ybr238c*Δ mutant was compared with that of the wild type (Figure S3A). Applying standard significance criteria, we found 322 genes up- and 56 genes down-regulated in the *ybr238c*Δ mutant compared to wild type (Figure S3B; Additional File 3). Thus, the transcriptome of the *ybr238c*Δ mutant is very distinct from that of the wild type.

Notably, we see several major metabolic changes. For the *ybr238c*Δ mutant, genes in mitochondrial metabolic processes such as oxidative phosphorylation and aerobic respiration show predominant enrichment (Figures 2A and 2B; Additional File 3). Since *YBR238C* expression is regulated by TORC1 (Figures 1A and 1B), it is not surprising that we observe similarities in the profiles of upregulated DEGs for the *ybr238c*Δ mutant and for the case of treating the wild type with rapamycin (Figures S3C and S3D).

Next, we experimentally tested whether the transcriptome longevity signatures is associated with enhanced mitochondrial metabolism, whether the cellular energy level has gone up and cellular stress responses are induced with a switch to oxidative metabolism [44,45]. Indeed, our metabolic analysis revealed an increased ATP level in *ybr238c*Δ mutants compared to wild type cells (Figures 2C and 2D). Hence, the *ybr238c*Δ mutation rewires the cellular metabolism

to promote resource-saving ways of energy production as the up-regulated expression of OXPHOS machinery subunits truly boosts ATP synthesis in *ybr238c*Δ mutant cells.

The enhanced mitochondrial function in *ybr238c*Δ mutants does also improve the protection against reactive oxygen species (ROS). Among the 150 TFs that control the upregulated DEG of the *ybr238c*Δ mutant (Additional File 3), 13 TFs are significantly overrepresented within the upregulated DEGs (Additional File 3). Importantly, we found that the stress response controlling transcription factor *MSN4* is up-regulated in *ybr238c*Δ mutants (Figures 2E and 2F; S4A-S4B) [16,46]. Concomitantly, we found less ROS level in *ybr238c*Δ mutant compared to wild type cells (Figures 2G and 2H).

Notably, the transcription factor regulated activation of stress response pathways (thioredoxins, molecular chaperones, etc.) [47,48] and the switch from fermentation to respiration are associated with delayed cellular aging [44,45,49,50]. Our results show that the *ybr238c*Δ mutation triggers oxidative metabolism and stress protective machineries activation and, as a result increases CLS. Collectively, our findings reveal that *YBR238C* is a TORC1 regulated gene involved in mitochondrial function coupled with cellular aging. Therefore, we refer to *YBR238C* as AAG1: Aging Associated Gene 1.

**_YBR238C_ negatively regulates mitochondrial function via _HAP4_-dependent and -independent mechanisms**

*HAP4* is a transcription factor that controls the expression of mitochondrial electron transport chain components including OXPHOS genes [46]. *HAP4* activity has been shown to increase lifespan by enhancing the mitochondrial respiration in cells [46]. Intriguingly, *HAP4* is among the 13 TFs overrepresented among the upregulated DEGs in *ybr238c*Δ mutant (Figures 3A-3C; Additional File 3). Consistent with these findings, transcription profile of mitochondrial genes in the *ybr238c*Δ mutant is opposite to that of the *hap4*Δ mutant (Figure 3D). For example, ETC complexes I – V genes' expression is increased in *ybr238c*Δ, however, it is decreased by *HAP4* deletion (Figure 3D).

We found that deletion of *HAP4* moderately decreases CLS at the background of the *ybr238c*Δ mutant (Figure 3E). To confirm that the decrease in lifespan is through the *HAP4* pathway, we examined the expression of mitochondrial respiratory genes. We found that *HAP4* deletion significantly decrease the ETC complex I – V genes' expression in *ybr238c*Δ mutant (Figure

3D). To note, *HAP4* deletion at the wild-type background decreases the cellular lifespan even more (Figure 3E), which is consistent with more dramatic reduction of ETC complexes I – V genes' expression (Figure 3D). Taken together these data suggests that *YBR238C* negatively regulates the *HAP4* activity. *HAP4*-upregulated, increased mitochondrial function contributes to the prolonged lifespan of *ybr238c*Δ mutants.

*YBR238C* gene deletion rescues some loss of lifespan of *hap4*Δ mutants (Figure 3F). The effect is especially pronounced until day 8 when wild-type cells are essentially 100% surviving. Yet, complete epistasis of phenotypes is not achieved. This observation parallels the above findings that *HAP4* deletion in *ybr238c*Δ mutant does not fully recover the mitochondrial ETC complexes I – V genes' expression and CLS at day 9 compared to the wild-type background (Figures 3D and 3E). Together, these results indicate that *YBR238C* affects cellular lifespan via *HAP4*-dependent and -independent mechanisms.

To confirm the existence of *HAP4*-independent mechanisms, we examined the lifespan and transcriptome under conditions of *YBR238C* overexpression (*YBR238C-OE*). As expected, *YBR238C-OE* decreases the expression of *HAP4*, of mitochondrial ETC complexes I – V genes (Figure 3G) as well as the CLS (Figure 3H). Strikingly, the lifespan of *YBR238C-OE* cells was shorter than for *hap4*Δ mutants (Figure 3H). Thus, *HAP4*-independent mechanism does exist through which *YBR238C* also affects cellular aging (Figure 3I).

**The *YBR238C* paralogue *RMD9* deletion decreases the lifespan of cells**

In yeast *S. cerevisiae*, *YBR238C* has a paralogue *RMD9* that shares ∼45% amino acid identity [51]. Given that *YBR238C* activity is tightly coupled with the lifespan, we investigated the role of its paralogue *RMD9* in cellular aging. Surprisingly, we found that *RMD9* deletion has an effect opposite to *YBR238C* deletion and it shortens CLS (Figures 4A-4C; S5A-S5C).

*RMD9* is known to control the mitochondrial metabolism gene expression by stabilizing and processing of the mitochondrial mRNAs [39,51]. We asked whether *RMD9* deletion induces mitochondrial dysfunction that, therefore, causes accelerated cellular aging. We first tested the mitochondrial activity by allowing mutant cells to grow under respiratory conditions [52–54]. We found that *rmd9*Δ mutants could perform on glucose media but they failed to grow on glycerol as a carbon source (known to require functional mitochondria; Figures 4D; S5D). Our results are in line with previously observed dysfunctional mitochondria in *rmd9*Δ mutants [39,51] .

In control experiments, we found a similar growth defect phenotype on glycerol medium for cells deficient in *PET100* and *COX6* mitochondrial genes (Figures 4D; S5D) [54]. CLS of *pet100*Δ and *cox6*Δ mutants were reduced compared to wild type (Figures 4E-4G; S5E-S5G). We also found lowered ATP- and higher ROS-levels in *rmd9*Δ*, pet100*Δ*, cox6*Δ mutants compared to wild type cells (Figures 4H and S5H).

In contrast, long lived *ybr238c*Δ mutants efficiently grow on respiratory medium with high ATP- and low ROS-levels (Figures 4D and 4H; S5D and S5H). So far, the results indicate that deletion of *YBR238C* potentiates the mitochondrial function that, in turn, leads to CLS increase. Thus, *YBR238C* and its paralogue *RMD9* antagonistically affect mitochondrial function, CLS and cellular aging.

**_YBR238C_ affects the cellular lifespan via an _RMD9_-dependent mechanism**

Previously, *YBR238C* deletion was shown to increase the CLS via *HAP4*-dependent and -independent mechanisms (Figure 3) and to rescue some loss of CLS of the *hap4*Δ mutant by a *HAP4*-independent mechanism (Figures 3E and 3F). Here, we ask whether *YBR238C* deletion suppresses the shortened lifespan of *rmd9*Δ mutants. We examined the lifespan of double deletion *rmd9*Δ *ybr238c*Δ mutant and compared it with *rmd9*Δ. We found that the deletion of *YBR238C* largely failed to recover the lifespan of *rmd9*Δ mutant to wild type cells; however, it partially prevented their early cell death (Figures 5A-5C). These results show that *YBR238C* deletion increases the cellular lifespan via *RMD9*-dependent mechanisms. Also, we found that the *YBR238C* deletion results in increased ATP- and reduced ROS-levels in the *rmd9*Δ mutant (Figures 5D and 5E).

Intriguingly, we find *RMD9* expression up-regulated in *ybr238c*Δ and down-regulated in *YBR238C-OE* cells, respectively (Figure 5F). So, we asked whether *RMD9* expression change is transcriptionally coupled in cellular lifespan phenotypes. Remarkably, *RMD9* overexpression increases the lifespan of cells (Figures 5G-5I) as we would have predicted from the observed changes with the *YBR238C* deletion phenotype.

To know whether this CLS increase is contributed by enhanced mitochondrial function, we quantified the ATP level in wild type, *YBR238C-OE,* and *RMD9-OE* cells. ATP level is higher in *RMD9-OE* cells than wild-type cells, a result in line with *RMD9* positively regulating

mitochondrial activity (Figure 5J). Consistent with the above findings, *YBR238C* overexpression decreases the ATP level (Figure 5J). Next, we assessed the oxidative stress and found that the ROS level in *RMD9-OE* cells was comparable to wild type. Yet, *YBR238C* overexpression increases the ROS level (Figure 5K).

It can be shown that the effects of *YBR238C* and *RMD9* are at least partially realized via the mitochondrial ETC pathway. Antimycin A (AMA) is an inhibitor of the ETC complex III, decreasing ATP synthesis (Figure S6A) [55]. Also, AMA treatment reduces the lifespan of cells (Figure S6B), confirming that mitochondrial energy supply is critical to delay cellular aging. Since *YBR238C* and *RMD9* affect the ATP level, we tested the AMA effect on their deletion and overexpression strains. We found that *ybr238c*Δ and *RMD9-OE* cells with their enhanced mitochondrial function phenotype were largely resistant to AMA treatment (Figure 5L). AMA aggravates the cellular aging of mitochondrial defective *YBR238C-OE* cells (Figure 5L). Notably, mitochondrial defective *rmd9*Δ cells were not further affected by AMA treatment (Figure 5L).

Altogether, our findings reveal that *YBR238C* affects CLS and cellular aging via modulating mitochondrial function by mechanisms including *HAP4-* and *RMD9*-dependent pathways (Figure 5M).

**_YBR238C_ connects TORC1 signaling with modulating mitochondrial function and cellular aging**

So far, we learned that *YBR238C* is regulated by TORC1 (Figures 1A and 1B) and it affects cellular lifespan by modulating mitochondrial function. Here, we wish establish the direct connection between the TORC1 signaling and mitochondrial activity. We treated cells with the TORC1 inhibitor rapamycin and found that, subsequently, the ATP level increases in the cells (Figures 6A; S6C). To test whether TORC1 affects mitochondrial function via *YBR238C*, we analyse the expression profile of mitochondrial ETC genes. As expected, rapamycin supplementation decreased the expression of *YBR238C* (Figures S6D and S6E) but induced the expression of ETC genes (Figure 6B). Remarkably, rapamycin-induced changes in the expression of ETC genes were largely unaffected in *ybr238c*Δ cells and reduced in *YBR238C-OE* cells (Figure 6B). Our results are consistent with the hypothesis that TORC1 regulates the mitochondrial ETC genes via *YBR238C*.

The strains *ybr238c*Δ and *YBR238C-OE* are associated with increased and decreased CLS, respectively. So, we ask whether TORC1 influences cellular aging via *YBR238C* by modulating mitochondrial function. We examined the effect of rapamycin supplementation on the lifespan of *ybr238c*Δ and *YBR238C-OE* cells. Strikingly, addition of rapamycin does not further increase CLS of *ybr238c*Δ cells. Additionally, anti-aging effect of rapamycin is significantly reduced in *YBR238C-OE* cells (Figure 6C). These findings are consistent with the rapamycin effect on transcriptomics profiles of ETC genes in *ybr238c*Δ and *YBR238C-OE* cells (Figure 6B). Taken together, these results reveal that *YBR238C* is a downstream effector of TORC1 signaling, connecting mitochondrial function for the regulation of cellular aging.

**Mitochondrial dysfunction induces the TORC1 activity that causes accelerated cellular aging**

We showed that *YBR238C-OE* cells are associated with mitochondrial dysfunction and shortened lifespan (Figure 5). Apparently, the accelerated cellular aging phenotype is primarily due to compromised cellular energy level that affects the lifespan. Genetic (*ybr238c*Δ) and chemical (rapamycin) mediated enhancement of ATP level increases the lifespan of wild type cells validate this conclusion. Notably, the rapamycin supplementation significantly rescued the shortened lifespan of mitochondrial defective *YBR238C-OE* cells (Figures 6D; and S6F). This observation suggests that, as a reaction on sensing mitochondrial dysfunction, TORC1 is activated which, in turn, leads to accelerated cellular aging. Indeed, we found that cellular growth (a proxy for TORC1 activity) of mitochondria dysfunctional *YBR238C-OE* cells was resistant to rapamycin inhibition at concentrations that were effective for wild type cells (Figure S6G).

Further, we asked what the effect of TORC1 activity under enhanced mitochondrial function conditions would be. To test this, we assessed the growth of *ybr238c*Δ cells with rapamycin. We found that the cellular growth of *ybr238c*Δ cells was reduced by rapamycin compared to wild type cells (Figure S6G). Apparently, TORC1 activity is not signalled downstream under these conditions and rapamycin further aggravates this by TORC1 inhibition. This result suggests that *YBR238C* affects TORC1 activity via modulating mitochondrial function.

We found a similar pattern of rapamycin effect on growth of mutant cells with enhanced or damaged mitochondrial function. Growth of *RMD9-OE* cells having enhanced mitochondrial function was sensitive to rapamycin (Figure S6G). Likewise, growth of defective

mitochondrial *rmd9*Δ, *pet100*Δ and *cox6*Δ mutants is resistant to rapamycin compared to wild type (Figure S6G). The *YBR238C* deletion reduced the rapamycin growth resistance phenotype of mitochondrial dysfunctional *rmd9*Δ (Figure S6G) and *hap4*Δ cells (Figure S6H), apparently by enabling enhanced mitochondrial function.

Taken together, we see that *YBR238C* plays a junction role in integrating mitochondrial function and TORC1 signaling.

**TORC1 inhibition prevents accelerated cellular aging caused by mitochondrial dysfunction in yeast and human cells**

Mitochondrial dysfunction increases the TORC1 activity and, subsequently, causes accelerating cellular aging. We asked whether inhibition of TORC1 activity could prevent accelerating cellular aging even under mitochondrial dysfunction conditions. Previously, we have already shown that rapamycin-mediated TORC1 inhibition partly rescued the shortened lifespan of mitochondrial defective *YBR238C-OE* cells (Figures 6D; and S6F). We examined other mitochondrial dysfunctional conditions to confirm that suppressive effect of rapamycin is not only specific to *YBR238C-OE*. We tested defective mitochondrial mutants *rmd9*Δ, *pet100*Δ and *cox6*Δ. In all cases, rapamycin supplementation prevents the accelerated cellular aging (Figures 6E-6G).

Rapamycin supplementation also rescued the AMA-mediated accelerated cellular aging (Figure 6H). We also quantified the ATP level to confirm that the suppressive effect of rapamycin is specific to mitochondrial function. Rapamycin supplementation increases the ATP level of AMA-treated cells (Figures 6I; and S6I), demonstrating that TORC1 inhibition improves mitochondrial function and thus suppresses accelerated cellular aging.

We further verified the connection of TORC1 and mitochondrial function in human cells. First, we examined the effect of AMA on the survival of HEK293 cells. AMA treatment decreases the viability of HEK293 cells (Figure 6J). Cell survival reduction is due to the mitochondrial dysfunction as we see lower ATP levels in AMA treated cells compared to untreated control (Figure S6J). Subsequently, we examined the survival of AMA-treated HEK293 cells with or without rapamycin supplementation. Rapamycin supplementation suppresses AMA-mediated cellular death (Figure 6K). Further rapamycin supplementation increases the ATP level treated cells (Figure S6J).

Our findings convincingly support that TORC1 inhibition suppresses cellular aging associated with mitochondrial dysfunction across species.

## DISCUSSION

Identifying lifespan regulators, genetic networks, and connecting genetic nodes relevant to cellular aging provides functional insight into the complexity of aging biology [1,7,11] for the subsequent design of anti-aging interventions. In this study, we first summarized literature and genome database reports about genes affecting aging in the yeast model (mostly observed in gene deletion screens). We found that AAGs (Aging Associated Genes) make up about one-third of the total yeast genome (many of them are functionally uncharacterized) and can be classified into 15 categories for increase/decrease CLS and/or RLS under various conditions.

We compared the set of AAGs with the group of RRGs (Rapamycin Regulated Genes) and found that about one third of the AAGs is TORC1 activity regulated. Among the functionally uncharacterized genes in this overlap set, the gene *YBR238C* stands out as the only one that (1) is downregulated by rapamycin and (2) its deletion increases both CLS [40] and RLS [8,41–43]. Thus, *YBR238C* is important among identified rapamycin-downregulated uncharacterized genes in AAG categories as it seems to rationally connect the rapamycin-induced TORC1 inhibition with the increase of both CLS and RLS.

We observed that the CLS of *ybr238c*Δ cells is higher than for wild type, regardless of various aging experimental conditions tested in this study. Transcriptional analysis of *ybr238c*Δ cells identified a longevity signature including enhanced gene expression related to mitochondrial energy metabolism and stress response genes [9,46,56–59]. In contrast, *YBR238C-OE* cells display mitochondrial dysfunction leading to decreased lifespan. Together, these results reveal that TORC1 regulates the *YBR238C* expression which is linked to mitochondrial function and cellular lifespan.

The *YBR238C* paralogue *RMD9* has been previously shown to affect mitochondrial function [39,51]. Surprisingly, we observed an antagonism regarding the CLS phenotype of deletion/overexpression for *YBR238C* and *RMD9*. *YBR238C* overexpression and *RMD9* deletion confer defective mitochondrial function associated with accelerated cellular aging and decrease lifespan of cells. In contrast, *YBR238C* deletion and *RMD9* overexpression enhance

the mitochondrial function that increase the cells' longevity. Consistent with the identified negative regulatory role of *YBR238C* on mitochondrial function, deletion of this gene partially suppressed the accelerated aging of *rmd9*Δ cells and AMA-treated cells. We identified that *YBR238C* influences mitochondrial function and the CLS phenotype with contributions from *HAP4*- and *RMD9*-dependent mechanisms. As (i) one of *RMD9*'s molecular functions has been shown to stabilize certain (mitochondrial) mRNAs and (ii) *YBR238C* has a has a homologous pentatricopeptide repeat region, the two paralogues might differ in the sets of protected mRNAs with opposite outcome on cellular longevity.

TORC1 is the major controller of cellular metabolism that links environmental cues and signals for cellular growth and homeostasis. TORC1 upregulates anabolic processes such as *de novo* synthesis of proteins, nucleotides, lipids, and downregulates catabolic processes such as inhibition of autophagy [23,25]. Results of genetic interventions (*YBR238C* deletion and overexpression) and rapamycin treatment show that *YBR238C* is a downstream effector by which TORC1 modulates mitochondrial activity. Most importantly, we found that TORC1 inhibition increases the mitochondrial function via *YBR238C* and, thereby, extends cellular lifespan.

In turn, we find that dysfunctional mitochondria lead to TORC1 activation both in yeast and in human cells with accompanying onset of accelerated cellular aging. Our results are in line with a recent report about anabolic pathways enhancement and suppression of catabolic processes in cells with defective mitochondria [60]. On the other hand, TORC1 activity decreases under enhanced mitochondrial function environment. The cause of the mitochondrial dysfunction (whether due to deletion of a critical gene or pharmacological intervention) is irrelevant in this context. Nevertheless, despite the mitochondrial insufficiency background, inhibition of TORC1 (e.g., with rapamycin) can partially rescue the shortened cellular lifespan (Figures 6D-6H; and S6F).

Our work sheds light onto the questions (i) how mitochondrial dysfunction is linked to accelerated cellular aging and (ii) how TORC1 inhibition suppresses the mitochondrial dysfunction and prevents shortening lifespan. Apparently, mitochondrial dysfunction aberrantly signals to increase the TORC1 activity that leads to accelerated aging in cells. Remarkably, TORC1 inhibition can often suppress the accelerated cellular aging associated with impaired mitochondrial function. Yet, we found that growth of mutant strains with

dysfunctional mitochondria can be resistant despite TORC1 inhibition by rapamycin with concentrations effective in wild-type cells possibly due to the dramatic increase of TORC1 activity as in *YBR238C-OE*, *rmd9*Δ, *pet100*Δ, *cox6*Δ and *hap4*Δ cells (Figures S6G and S6H).

Our interpretation of the experimental results is supported by two recently published studies: (1) TORC1 activation was observed after mitochondrial ETC dysfunction in an induced pluripotent cell model [61]. (2) The inhibition of TORC1 delays the progression of brain pathology of mice with ETC complex I NDUFS4-subunit knockout [62].

We think that it will be insightful to explore TORC1 activity under various conditions with compromised mitochondrial function including mitochondrial fission and fusion dynamics which is reported to affect in cell viability [63,64]. Altogether, our findings uncover the central role of the feedback loop between mitochondrial function and TORC1 signaling (TORC1-MItochondria-TORC1 (TOMITO) signaling process). Whereas the effector from TORC1 to mitochondria involves *YBR238C*, the other direction appears executed via metabolite sensing (e.g., α-keto-glutarate, glutamine, etc.) [65].

## FIGURE LEGEND

**Figure 1. *YBR238C* deletion increases the cellular lifespan**

(A and B) Expression analysis of *YBR238C* gene by qRT-PCR in yeast *Saccharomyces cerevisiae* genetic backgrounds BY4743 (A) and CEN.PK113-7D (B). Data are represented as means ± SD (n=4). ****P < 0.0001 based on two-sided Student's t-test.

(C and D) Chronological lifespan (CLS) of the wild type and *ybr238c*Δ mutant was assessed in the SD medium supplemented with auxotrophic amino acids for BY4743 (C) and only the SD medium for CEN.PK113-7D (D) strains in 96-well plate. Aged cells survival was measured relative to the outgrowth of day 2. Data are represented as means ± SD (n=3) (C) and (n=4) (D). **P < 0.01, ***P < 0.001, and ****P < 0.0001 based on two-way ANOVA followed by Šídák's multiple comparisons test.

(E and F) CLS of the wild type and *ybr238c*Δ mutant was performed in the flask. Outgrowth was performed for ten-fold serial diluted aged cells onto the YPD agar plate (E) and YPD medium in the 96-well plate (F). The serial outgrowth of aged cells on agar medium was imaged (E) and quantified the survival relative to outgrowth of day 2 (F). A representative of two experiments for (E) and (F) is shown.

**Figure 2. Longevity signatures of *ybr238c*Δ mutant**

(A and B) Functional enrichment analysis of upregulated genes in yeast *Saccharomyces cerevisiae ybr238c*Δ mutant compared to wild type (BY4743). Bar plots showing the enriched biological process (A) and identified MCODE complexes based on the top-three ontology enriched terms (B). See also Additional File 3.

(C and D) ATP analysis of wild type and *ybr238c*Δ mutant for BY4743 (C) and CEN.PK113-7D (D). Data are represented as means ± SD (n=6). **P < 0.01, and ****P < 0.0001 based on two-sided Student's t-test.

(E and F) Expression analysis of *MSN4* gene by qRT-PCR in yeast *Saccharomyces cerevisiae* genetic backgrounds BY4743 (E) and CEN.PK113-7D (F). Data are represented as means ± SD (n=2). **P < 0.01 based on two-sided Student's t-test.

(G and H) ROS analysis of wild type and *ybr238c*Δ mutant for BY4743 (G) and CEN.PK113-7D (H). Data are represented as means ± SD (n=4). ***P < 0.001, and ****P < 0.0001 based on two-sided Student's t-test.

**Figure 3. *YBR238C* affects cellular aging via *HAP4*-dependent and independent mechanisms**

(A) The *HAP4* regulon within the upregulated DEGs of *ybr238c*Δ mutant. See also Additional File 3.

(B and C) Expression analysis of *HAP4* gene by qRT-PCR in yeast *Saccharomyces cerevisiae* genetic backgrounds BY4743 (B) and CEN.PK113-7D (C). Data are represented as means ± SD (n=2). **P < 0.01 based on two-sided Student's t-test.

(D) Heatmap of mitochondrial ETC genes expression analysis by qRT-PCR in CEN.PK113-7D strains. Data are represented as means ± SD (n=2).

(E, F and H) Chronological lifespan (CLS) of yeast *Saccharomyces cerevisiae* genetic background CEN.PK113-7D strains was performed in the SD medium in 96-well plate. Aged cells survival was measured relative to the outgrowth of day 2. Data are represented as means ± SD (n=6). *P < 0.05, ***P < 0.001, ****P < 0.0001 and ns: non-significant. Ordinary one-way ANOVA followed by Tukey's multiple comparisons test (E and F). Two-way ANOVA followed by Šídák's multiple comparisons test (H).

(G) Expression analysis of *HAP4* and ETC genes by qRT-PCR in *YBR238C* deletion (*ybr238c*Δ) and overexpression (*YBR238C-OE*) strains of yeast *Saccharomyces cerevisiae* genetic background CEN.PK113-7D (C). Data are represented as means ± SD (n=2). **P < 0.01, ***P < 0.001 and ****P < 0.000 based on Two-way ANOVA followed by Šídák's multiple comparisons test.

(I) Model representing regulation of cellular aging by *YBR238C* via *HAP4*- dependent and independent mechanisms.

**Figure 4. *RMD9* deletion decreases the cellular lifespan**

(A and E) Chronological lifespan (CLS) of yeast *Saccharomyces cerevisiae* genetic background CEN.PK113-7D strains was performed in the SD medium in 96-well plate. Aged cells survival was measured relative to the outgrowth of day 2. Data are represented as means ± SD (n=12) (A) and (n=6) (B). ****P < 0.0001 and ns: non-significant. Ordinary one-way ANOVA followed by Tukey's multiple comparisons test (A). Two-way ANOVA followed by Dunnett's multiple comparisons test (E).

(B, C, F and G) CLS of yeast strains was performed in the flask. Outgrowth was performed for ten-fold serial diluted aged cells onto the YPD agar plate (B and F) and YPD medium in the 96-well plate (C and G). The serial outgrowth of aged cells on agar medium was imaged (B and F) and quantified the survival relative to outgrowth of day 1 (C and G). A representative of two experiments for B, C, F and G is shown.

(D) Serial dilution growth assays of the yeast strains on fermentative glucose medium (YPD) and respiratory glycerol medium (YPG).

(H) ATP level in yeast strains. Data are represented as means ± SD (n=3). *P < 0.05, and ***P < 0.001 based on ordinary one-way ANOVA followed by Dunnett's multiple comparisons test.

See also Figure S5.

**Figure 5. *YBR238C* affects cellular aging via *RMD9*- dependent mechanism**

(A, B, G and H) Chronological lifespan (CLS) of yeast *Saccharomyces cerevisiae* genetic background CEN.PK113-7D strains was performed in the SD medium in the flask. Outgrowth was performed for ten-fold serial diluted aged cells onto the YPD agar plate (A and G) and YPD medium in the 96-well plate (B and H). The serial outgrowth of aged cells on agar medium was imaged (A and G) and quantified the survival relative to outgrowth of day 2 (B and H). A representative of two experiments for A, B, G and H is shown.

(C and I) CLS of yeast strains was performed in the SD medium in 96-well plate. Aged cells survival was measured relative to the outgrowth of day 2. Data are represented as means ± SD (n=6) (C) and (n=12) (I). ****P < 0.0001 based on two-way ANOVA followed by Tukey's multiple comparisons test (C) and Dunnett's multiple comparisons test (I). ns: non-significant.

(D and J) ATP level in yeast strains. Data are represented as means ± SD (n=4). *P < 0.05, ***P < 0.001, and ****P < 0.0001 based on on ordinary one-way ANOVA followed by Tukey's multiple comparisons test.

(E and K) ROS level in yeast strains. Data are represented as means ± SD (n=4). **P < 0.01, ***P < 0.001, and ****P < 0.0001 based on ordinary one-way ANOVA followed by Tukey's multiple comparisons test. ns: non-significant.

(F) Expression analysis of *RMD9* gene by qRT-PCR in yeast strains. Data are represented as means ± SD (n=4). ***P < 0.001, and ****P < 0.0001 based on ordinary one-way ANOVA followed by Tukey's multiple comparisons test.

(L) Effect of antimycin A (AMA) treatment on CLS of yeast strain was assessed in 96-well plate. Aged cells survival was measured relative to the outgrowth of day 1. A representative heatmap data of three experiments is shown.

(M) Model representing regulation of cellular aging by *YBR238C* via *HAP4* and *RMD9* dependent mechanisms.

**Figure 6. TORC1-MItochondria-TORC1 (TOMITO) signaling axis regulate cellular aging**

(A) ATP analysis of logarithmic phase wild type CEN.PK113-7D yeast cells treated with rapamycin for 1 hour. Data are represented as means ± SD (n=3). ****P < 0.0001 based on ordinary one-way ANOVA followed by Dunnett's multiple comparisons test. See also Figure S5C.

(B) Expression analysis of mitochondrial ETC genes by qRT-PCR. Data are represented as means ± SD (n=2).

(C-G) Chronological lifespan (CLS) of yeast strains with indicated concentrations of rapamycin was performed in the SD medium in 96-well plate. Aged cells survival was measured relative to the outgrowth of day 2. Data are represented as means ± SD (n=3). ***P

< 0.001, and ****P < 0.0001 based on two-way ANOVA followed by Dunnett's multiple comparisons test. ns: non-significant.

(H) CLS of wild type yeast strain with indicated concentrations of rapamycin and antimycin A (10 µM) was performed in the SD medium in 96-well plate. Aged cells survival was measured relative to the outgrowth of day 1. Data are represented as means ± SD (n=3). ****P < 0.0001 based on two-way ANOVA followed by Dunnett's multiple comparisons test. ns: non-significant. ns: non-significant.

(I) ATP analysis of stationary phase wild type CEN.PK113-7D yeast cells were incubated with rapamycin (10 nM) and antimycin A (10 µM). Data are represented as means ± SD (n=6). ****P < 0.0001 based on ordinary one-way ANOVA followed by Tukey's multiple comparisons test. See also Figure S6H.

(J) Determination of human HEK293 cells survival incubated with indicated concentrations of antimycin A for 6 days. Untreated control is considered 100% cell survial. Data are represented as means ± SD (n=6).

(K) Heatmap for cell survival analysis of human HEK293 cells incubated with indicated concentrations of antimycin A and rapamycin for 6 days. Cell viability at antimycin A and rapamycin combination concentrations was measured relative to their individual treated concentration.  A representative data of two experiments is shown.

**Table 1. Numbers of known aging associated genes (AAGs) reported in the scientific literature to affect (increase/decrease CLS/RLS) under a variety of conditions**

The gene lists were extracted, after processing, from downloaded files (as of 8th November 2022) using the databases SGD [19] and GenAge [20]. The actual gene lists are available in Additional File 1'. The signs '+' and '-' indicate that the respective annotation property is present or missing in that group of genes. We present the total number of genes in each category as the number of, as a trend, severely understudied/uncharacterized genes among those. The columns 'RUG' and 'RDG' show the numbers of rapamycin-up- and -downregulated genes in each of the 15 categories.

| category | CLS increase | CLS decrease | RLS increase | RLS decrease | Number of genes | Understudied genes | RUG | RDG |
|---|---|---|---|---|---|---|---|---|
| 1 | + | - | - | - | 328 | 20 | 68 | 62 |
| 2 | - | + | - | - | 615 | 22 | 108 | 73 |
| 3 | - | - | + | - | 349 | 19 | 73 | 64 |
| 4 | - | - | - | + | 318 | 15 | 43 | 56 |
| 5 | + | + | - | - | 108 | 0 | 17 | 18 |
| 6 | + | - | + | - | 72 | 2 | 12 | 26 |
| 7 | + | - | - | + | 72 | 3 | 9 | 18 |
| 8 | - | + | + | - | 120 | 3 | 14 | 28 |
| 9 | - | + | - | + | 180 | 0 | 24 | 34 |
| 10 | - | - | + | + | 59 | 0 | 8 | 14 |
| 11 | + | + | + | - | 29 | 1 | 7 | 7 |
| 12 | + | + | - | + | 45 | 1 | 7 | 9 |
| 13 | + | - | + | + | 30 | 1 | 2 | 11 |
| 14 | - | + | + | + | 55 | 1 | 5 | 11 |
| 15 | + | + | + | + | 19 | 0 | 0 | 2 |

## STAR METHODS

Detailed methods are provided in this paper and include the following:

- **KEY RESOURCES TABLE**
- **LEAD CONTACT AND MATERIALS AVAILABILITY**
- **EXPERIMENTAL MODEL AND SUBJECT DETAILS**
  - Yeast strains, growth media and cell culture
  - Human cell lines, growth media and cell culture
  - Chemical treatment to cell culture
- **METHOD DETAILS**
  - Data acquisition
  - Aging associated gene analysis
  - Yeast aging assay
  - RNA extraction
  - RNA sequencing and bioinformatics analysis
  - qRT-PCR analysis
  - ATP analysis
  - Transcription factors analysis
  - ROS measurement
  - Fermentative and respiratory growth assay
  - Growth sensitivity assay
- **QUANTIFICATION AND STATISTICAL ANALYSIS**
- **DATA AVAILABILITY**

## SUPPLEMENTAL INFORMATION

Supplemental information includes six figures and three additional supplementary information.

## FUNDING

This work was supported by Bioinformatics Institute (BII), A*STAR Career Development Fund (C210112008) and the Global Healthy Longevity Catalyst Awards grant (MOH-000758–00).

## AUTHOR CONTRIBUTIONS STATEMENT

Mohammad Alfatah: Conceiving of the project, Writing, Editing and Funding Acquisition

Jolyn Lim Jia Jia: Methodology, Investigation, Bioinformatics, Formal analysis, and Reviewing

Yizhong Zhnag: Methodology, Investigation, Formal analysis, and Reviewing

Arshia Naaz: Methodology, Formal analysis, Investigation and Reviewing

Trishia Cheng Yi Ning: Methodology, Formal analysis, Investigation and Reviewing

Sonia Yogasundaram: Methodology, Investigation and Reviewing

Nashrul Afiq Faidzinn: Methodology, Investigation and Reviewing

Jovian Lin Jing: Methodology, Investigation and Reviewing

Birgit Eisenhaber: Methodology, Investigation, Bioinformatics, Formal analysis and Reviewing

Frank Eisenhaber: Investigation, Bioinformatics, Formal analysis, Reviewing, Editing and Funding Acquisition

## ACKNOWLEDGMENTS

We thank Dr. Maurer-Stroh Sebastian, Dr. Lee Hwee Kuan and Dr. Chandra S Verma for backing this research.

## DECLARATION OF INTERESTS

The authors declare no competing interests.

## REFERENCES


1. Kennedy, B.K., Berger, S.L., Brunet, A., Campisi, J., Cuervo, A.M., Epel, E.S., Franceschi, C., Lithgow, G.J., Morimoto, R.I., Pessin, J.E., et al. (2014). Geroscience: Linking aging to chronic disease. Cell *159*, 709–713. 10.1016/j.cell.2014.10.039.
2. Atzmon, G., Marotta, F., Kyriazis, M., Santoro, A., Franceschi, C., Garagnani, P., Morsiani, C., Conte, M., Grignolio, A., Monti, D., et al. (2018). The Continuum of Aging and Age-Related Diseases: Common Mechanisms but Different Rates. Article *5*, 1. 10.3389/fmed.2018.00061.
3. Tchkonia, T., and Kirkland, J.L. (2018). Aging, Cell Senescence, and Chronic Disease: Emerging Therapeutic Strategies. JAMA *320*, 1319–1320. 10.1001/JAMA.2018.12440.
4. Gladyshev, V.N. (2016). Aging: progressive decline in fitness due to the rising deleteriome adjusted by genetic, environmental, and stochastic processes. Aging Cell *15*, 594–602. 10.1111/acel.12480.
5. Richardson, A. (2021). You have come a long way baby: Five decades of research on the biology of aging from the perspective of a researcher studying aging. Journals Gerontol. - Ser. A Biol. Sci. Med. Sci. *76*, 57–63. 10.1093/GERONA/GLAA208.
6. Cao, X., Li, W., Wang, T., Ran, D., Davalos, V., Planas-Serra, L., Pujol, A., Esteller, M., Wang, X., and Yu, H. (2022). Accelerated biological aging in COVID-19 patients. Nat. Commun. *13*, 13. 10.1038/s41467-022-29801-8.
7. Cohen, A.A., Ferrucci, L., Fülöp, T., Gravel, D., Hao, N., Kriete, A., Levine, M.E., Lipsitz, L.A., Olde Rikkert, M.G.M., Rutenberg, A., et al. (2022). A complex systems approach to aging biology. Nat. Aging *2*, 580–591. 10.1038/s43587-022-00252-6.
8. McCormick, M.A., Delaney, J.R., Tsuchiya, M., Tsuchiyama, S., Shemorry, A., Sim, S., Chou, A.C.Z., Ahmed, U., Carr, D., Murakami, C.J., et al. (2015). A Comprehensive Analysis of Replicative Lifespan in 4,698 Single-Gene Deletion Strains Uncovers Conserved Mechanisms of Aging. Cell Metab. *22*, 895–906. 10.1016/j.cmet.2015.09.008.
9. Powers, R.W., Kaeberlein, M., Caldwell, S.D., Kennedy, B.K., and Fields, S. (2006). Extension of chronological life span in yeast by decreased TOR pathway signaling. Genes Dev. 10.1101/gad.1381406.
10. Hamilton, B., Dong, Y., Shindo, M., Liu, W., Odell, I., Ruvkun, G., and Lee, S.S. (2005). A systematic RNAi screen for longevity genes in C. elegans. Genes Dev. *19*,

1544–1555. 10.1101/gad.1308205.

11. López-Otín, C., Blasco, M.A., Partridge, L., Serrano, M., and Kroemer, G. (2013). The hallmarks of aging. Cell *153*, 1194–1217. 10.1016/j.cell.2013.05.039.
12. López-Otín, C., Blasco, M.A., Partridge, L., Serrano, M., and Kroemer, G. (2023). Hallmarks of aging: An expanding universe. Cell *186*, 243–278. 10.1016/J.CELL.2022.11.001.
13. Partridge, L., Fuentealba, M., and Kennedy, B.K. (2020). The quest to slow ageing through drug discovery. Nat. Rev. Drug Discov. 10.1038/s41573-020-0067-7.
14. Singh, P.P., Demmitt, B.A., Nath, R.D., and Brunet, A. (2019). The Genetics of Aging: A Vertebrate Perspective. Cell *177*, 200–220. 10.1016/J.CELL.2019.02.038.
15. Longo, V.D., and Fabrizio, P. (2015). Chronological aging in Saccharomyces cerevisiae. Subcell. Biochem. *57*, 101–121. 10.1007/978-94-007-2561-4_5.
16. Longo, V.D., Shadel, G.S., Kaeberlein, M., and Kennedy, B. (2012). Replicative and chronological aging in saccharomyces cerevisiae. Cell Metab. 10.1016/j.cmet.2012.06.002.
17. Fontana, L., Partridge, L., and Longo, V.D. (2010). Extending Healthy Life Span—From Yeast to Humans. Science (80-. ). *328*, 321–326. 10.1126/science.1172539.
18. Zimmermann, A., Hofer, S., Pendl, T., Kainz, K., Madeo, F., and Carmona-Gutierrez, D. (2018). Yeast as a tool to identify anti-aging compounds. FEMS Yeast Res. *18*. 10.1093/femsyr/foy020.
19. Engel, S.R., Wong, E.D., Nash, R.S., Aleksander, S., Alexander, M., Douglass, E., Karra, K., Miyasato, S.R., Simison, M., Skrzypek, M.S., et al. (2022). New data and collaborations at the Saccharomyces Genome Database: updated reference genome, alleles, and the Alliance of Genome Resources. Genetics *220*. 10.1093/genetics/iyab224.
20. William Townes, F., Carr, K., and Miller, J.W. (2020). Identifying longevity associated genes by integrating gene expression and curated annotations. PLoS Comput. Biol. *16*. 10.1371/journal.pcbi.1008429.
21. Sherman, B.T., Hao, M., Qiu, J., Jiao, X., Baseler, M.W., Lane, H.C., Imamichi, T., and Chang, W. (2022). DAVID: a web server for functional enrichment analysis and functional annotation of gene lists (2021 update). Nucleic Acids Res. *50*, W216–W221. 10.1093/nar/gkac194.
22. Loewith, R., and Hall, M.N. (2011). Target of rapamycin (TOR) in nutrient signaling and growth control. Genetics *189*, 1177–1201. 10.1534/genetics.111.133363.

23. Saxton, R.A., and Sabatini, D.M. (2017). mTOR signaling in growth, metabolism, and disease. Cell *168*, 960–976.
24. Liu, G.Y., and Sabatini, D.M. (2020). mTOR at the nexus of nutrition, growth, ageing and disease. Nat. Rev. Mol. Cell Biol. *21*, 1–21. 10.1038/s41580-019-0199-y.
25. González, A., and Hall, M.N. (2017). Nutrient sensing and TOR signaling in yeast and mammals. EMBO J. *36*, 397–408. 10.15252/embj.201696010.
26. Bitto, A., Ito, T.K., Pineda, V. V., Letexier, N.J., Huang, H.Z., Sutlief, E., Tung, H., Vizzini, N., Chen, B., Smith, K., et al. (2016). Transient rapamycin treatment can increase lifespan and healthspan in middle-aged mice. Elife. 10.7554/eLife.16351.
27. Johnson, S.C., Rabinovitch, P.S., and Kaeberlein, M. (2013). MTOR is a key modulator of ageing and age-related disease. Nature. 10.1038/nature11861.
28. Selvarani, R., Mohammed, S., and Richardson, A. (2021). Effect of rapamycin on aging and age-related diseases—past and future. GeroScience. 10.1007/s11357-020-00274-1.
29. Wilkinson, J.E., Burmeister, L., Brooks, S. V., Chan, C.C., Friedline, S., Harrison, D.E., Hejtmancik, J.F., Nadon, N., Strong, R., Wood, L.K., et al. (2012). Rapamycin slows aging in mice. Aging Cell. 10.1111/j.1474-9726.2012.00832.x.
30. Li, J., Kim, S.G., and Blenis, J. (2014). Rapamycin: One drug, many effects. Cell Metab. 10.1016/j.cmet.2014.01.001.
31. Zhang, Y., Zhang, J., and Wang, S. (2021). The Role of Rapamycin in Healthspan Extension via the Delay of Organ Aging. Ageing Res. Rev. 10.1016/j.arr.2021.101376.
32. Ramos, F.J., Chen, S.C., Garelick, M.G., Dai, D.F., Liao, C.Y., Schreiber, K.H., MacKay, V.L., An, E.H., Strong, R., Ladiges, W.C., et al. (2012). Rapamycin reverses elevated mTORC1 signaling in lamin A/C-deficient mice, rescues cardiac and skeletal muscle function, and extends survival. Sci. Transl. Med. 10.1126/scitranslmed.3003802.
33. Alfatah, M., and Eisenhaber, F. (2023). The PICLS high-throughput screening method for agents extending cellular longevity identifies 2,5-anhydro-D-mannitol as novel anti-aging compound. GeroScience *45*, 141–158. 10.1007/s11357-022-00598-0.
34. Gowans, G.J., Schep, A.N., Wong, K.M., King, D.A., Greenleaf, W.J., and Morrison, A.J. (2018). INO80 Chromatin Remodeling Coordinates Metabolic Homeostasis with Cell Division. Cell Rep. *22*, 611–623. 10.1016/j.celrep.2017.12.079.
35. Alfatah, M., Wong, J.H., Krishnan, V.G., Lee, Y.C., Sin, Q.F., Goh, C.J.H., Kong, K.W., Hoon, S., Arumugam, P., Lee, W.T., et al. (2021). TORC1 regulates the

transcriptional response to glucose and developmental cycle via the Tap42-Sit4-Rrd1/2 pathway in Saccharomyces cerevisiae. BMC Biol., 859793. 10.1186/s12915-021-01030-3.

36. Huh, W.K., Falvo, J. V., Gerke, L.C., Carroll, A.S., Howson, R.W., Weissman, J.S., and O'Shea, E.K. (2003). Global analysis of protein localization in budding yeast. Nature *425*, 686–691. 10.1038/nature02026.

37. Eisenhaber, B., Kuchibhatla, D., Sherman, W., Sirota, F.L., Berezovsky, I.N., Wong, W.C., and Eisenhaber, F. (2016). The recipe for protein sequence-based function prediction and its implementation in the ANNOTATOR software environment. In Methods in Molecular Biology (Methods Mol Biol), pp. 477–506. 10.1007/978-1-4939-3572-7_25.

38. Zimmermann, L., Stephens, A., Nam, S.Z., Rau, D., Kübler, J., Lozajic, M., Gabler, F., Söding, J., Lupas, A.N., and Alva, V. (2018). A Completely Reimplemented MPI Bioinformatics Toolkit with a New HHpred Server at its Core. J. Mol. Biol. *430*, 2237–2243. 10.1016/j.jmb.2017.12.007.

39. Hillen, H.S., Markov, D.A., Wojtas, I.D., Hofmann, K.B., Lidschreiber, M., Cowan, A.T., Jones, J.L., Temiakov, D., Cramer, P., and Anikin, M. (2021). The pentatricopeptide repeat protein Rmd9 recognizes the dodecameric element in the 3′-UTRs of yeast mitochondrial mRNAs. Proc. Natl. Acad. Sci. U. S. A. *118*. 10.1073/pnas.2009329118.

40. Burtner, C.R., Murakami, C.J., Olsen, B., Kennedy, B.K., and Kaeberlein, M. (2011). A genomic analysis of chronological longevity factors in budding yeast. Cell Cycle *10*, 1385–1396. 10.4161/cc.10.9.15464.

41. Delaney, J.R., Sutphin, G.L., Dulken, B., Sim, S., Kim, J.R., Robison, B., Schleit, J., Murakami, C.J., Carr, D., An, E.H., et al. (2011). Sir2 deletion prevents lifespan extension in 32 long-lived mutants. Aging Cell *10*, 1089–1091. 10.1111/j.1474-9726.2011.00742.x.

42. Kaeberlein, M., Powers, R.W., Steffen, K.K., Westman, E.A., Hu, D., Dang, N., Kerr, E.O., Kirkland, K.T., Fields, S., and Kennedy, B.K. (2005). Cell biology: Regulation of yeast replicative life span by TOR and Sch9 response to nutrients. Science (80-. ). *310*, 1193–1196. 10.1126/science.1115535.

43. Schleit, J., Johnson, S.C., Bennett, C.F., Simko, M., Trongtham, N., Castanza, A., Hsieh, E.J., Moller, R.M., Wasko, B.M., Delaney, J.R., et al. (2013). Molecular mechanisms underlying genotype-dependent responses to dietary restriction. Aging

Cell *12*, 1050–1061. 10.1111/acel.12130.

44. Petti, A.A., Crutchfield, C.A., Rabinowitz, J.D., and Botstein, D. (2011). Survival of starving yeast is correlated with oxidative stress response and nonrespiratory mitochondrial function. Proc. Natl. Acad. Sci. U. S. A. *108*, E1089–E1098. 10.1073/PNAS.1101494108/SUPPL_FILE/SD01.XLSX.

45. Galluzzi, L., Kepp, O., Trojel-Hansen, C., and Kroemer, G. (2012). Mitochondrial control of cellular life, stress, and death. Circ. Res. *111*, 1198–1207. 10.1161/CIRCRESAHA.112.268946.

46. Lin, S.J., Kaeberlein, M., Andalis, A.A., Sturtz, L.A., Defossez, P.A., Culotta, V.C., Fink, G.R., and Guarente, L. (2002). Calorie restriction extends saccharomyces cerevisiae lifespan by increasing respiration. Nature *418*, 344–348. 10.1038/nature00829.

47. Turcotte, B., Liang, X.B., Robert, F., and Soontorngun, N. (2010). Transcriptional regulation of nonfermentable carbon utilization in budding yeast. FEMS Yeast Res. *10*, 2–13. 10.1111/j.1567-1364.2009.00555.x.

48. Schüller, H.J. (2003). Transcriptional control of nonfermentative metabolism in the yeast Saccharomyces cerevisiae. Curr. Genet. *43*, 139–160. 10.1007/s00294-003-0381-8.

49. Jensen, M.B., and Jasper, H. (2014). Mitochondrial proteostasis in the control of aging and longevity. Cell Metab. *20*, 214–225. 10.1016/j.cmet.2014.05.006.

50. Martínez-Reyes, I., and Chandel, N.S. (2020). Mitochondrial TCA cycle metabolites control physiology and disease. Nat. Commun. *11*. 10.1038/s41467-019-13668-3.

51. Nouet, C., Bourens, M., Hlavacek, O., Marsy, S., Lemaire, C., and Ve Dujardin, G. Rmd9p Controls the Processing/Stability of Mitochondrial mRNAs and Its Overexpression Compensates for a Partial Deficiency of Oxa1p in Saccharomyces cerevisiae. 10.1534/genetics.106.063883.

52. Hughes, C.E., Coody, T.K., Jeong, M.Y., Berg, J.A., Winge, D.R., and Hughes, A.L. (2020). Cysteine Toxicity Drives Age-Related Mitochondrial Decline by Altering Iron Homeostasis. Cell *180*, 296-310.e18. 10.1016/j.cell.2019.12.035.

53. Zulkifli, M., Neff, J.K., Timbalia, S.A., Garza, N.M., Chen, Y., Watrous, J.D., Murgia, M., Trivedi, P.P., Anderson, S.K., Tomar, D., et al. (2020). Yeast homologs of human MCUR1 regulate mitochondrial proline metabolism. Nat. Commun. *11*. 10.1038/s41467-020-18704-1.

54. Merz, S., and Westermann, B. (2009). Genome-wide deletion mutant analysis reveals

genes required for respiratory growth, mitochondrial genome maintenance and mitochondrial protein synthesis in Saccharomyces cerevisiae. Genome Biol. *10*, 95. 10.1186/gb-2009-10-9-r95.

55. Huang, L.S., Cobessi, D., Tung, E.Y., and Berry, E.A. (2005). Binding of the respiratory chain inhibitor antimycin to the mitochondrial bc1 complex: A new crystal structure reveals an altered intramolecular hydrogen-bonding pattern. J. Mol. Biol. *351*, 573–597. 10.1016/j.jmb.2005.05.053.
56. Sun, N., Youle, R.J., and Finkel, T. (2016). The Mitochondrial Basis of Aging. Mol. Cell. 10.1016/j.molcel.2016.01.028.
57. Navarro, A., and Boveris, A. (2007). The mitochondrial energy transduction system and the aging process. Am. J. Physiol. - Cell Physiol. *292*, 670–686. 10.1152/ajpcell.00213.2006.
58. Qiu, X., Brown, K., Hirschey, M.D., Verdin, E., and Chen, D. (2010). Cell Metabolism Calorie Restriction Reduces Oxidative Stress by SIRT3-Mediated SOD2 Activation. Cell Metab. *12*, 662–667. 10.1016/j.cmet.2010.11.015.
59. Bonawitz, N.D., Chatenay-Lapointe, M., Pan, Y., and Shadel, G.S. (2007). Reduced TOR Signaling Extends Chronological Life Span via Increased Respiration and Upregulation of Mitochondrial Gene Expression. Cell Metab. *5*, 265–277. 10.1016/j.cmet.2007.02.009.
60. Nikkanen, J., Forsström, S., Euro, L., Paetau, I., Kohnz, R.A., Wang, L., Chilov, D., Viinamäki, J., Roivainen, A., Marjamäki, P., et al. (2016). Mitochondrial DNA Replication Defects Disturb Cellular dNTP Pools and Remodel One-Carbon Metabolism. Cell Metab. *23*, 635–648. 10.1016/J.CMET.2016.01.019.
61. Zheng, X., Boyer, L., Jin, M., Kim, Y., Fan, W., Bardy, C., Berggren, T., Evans, R.M., Gage, F.H., and Hunter, T. (2016). Alleviation of neuronal energy deficiency by mtor inhibition as a treatment for mitochondria-related neurodegeneration. Elife *5*. 10.7554/eLife.13378.
62. Johnson, S.C., Yanos, M.E., Kayser, E.B., Quintana, A., Sangesland, M., Castanza, A., Uhde, L., Hui, J., Wall, V.Z., Gagnidze, A., et al. (2013). MTOR inhibition alleviates mitochondrial disease in a mouse model of Leigh syndrome. Science (80-. ). *342*, 1524–1528. 10.1126/science.1244360.
63. Archer, S.L. (2013). Mitochondrial Dynamics — Mitochondrial Fission and Fusion in Human Diseases. N. Engl. J. Med. *369*, 2236–2251. 10.1056/NEJMRA1215233/SUPPL_FILE/NEJMRA1215233_DISCLOSURES.PDF.

64. Youle, R.J., and Van Der Bliek, A.M. (2012). Mitochondrial fission, fusion, and stress. Science (80-. ). *337*, 1062–1065. 10.1126/science.1219855.

65. Durán, R. V., Oppliger, W., Robitaille, A.M., Heiserich, L., Skendaj, R., Gottlieb, E., and Hall, M.N. (2012). Glutaminolysis Activates Rag-mTORC1 Signaling. Mol. Cell *47*, 349–358. 10.1016/j.molcel.2012.05.043.

66. van Dijken JP, Bauer, J., Brambilla, L., Duboc, P., Francois, J., Gancedo, C., Giuseppin, M., Heijnen, J., Hoare, M., Lange, H., et al. (2000). An interlaboratory comparison of physiological and genetic properties of four Saccharomyces cerevisiae strains. Enzyme Microb. Technol. *26*, 706–714. 10.1016/s0141-0229(00)00162-9.

67. Longtine, M.S., McKenzie, A., Demarini, D.J., Shah, N.G., Wach, A., Brachat, A., Philippsen, P., and Pringle, J.R. (1998). Additional modules for versatile and economical PCR-based gene deletion and modification in Saccharomyces cerevisiae. Yeast *14*, 953–961. 10.1002/(SICI)1097-0061(199807)14:10<953::AID-YEA293>3.0.CO;2-U.

68. Teixeira, M.C., Monteiro, P., Jain, P., Tenreiro, S., Fernandes, A.R., Mira, N.P., Alenquer, M., Freitas, A.T., Oliveira, A.L., and Sá-Correia, I. (2006). The YEASTRACT database: a tool for the analysis of transcription regulatory associations in Saccharomyces cerevisiae. Nucleic Acids Res. 10.1093/nar/gkj013.

69. Teixeira, M.C., Monteiro, P.T., Palma, M., Costa, C., Godinho, C.P., Pais, P., Cavalheiro, M., Antunes, M., Lemos, A., Pedreira, T., et al. (2018). YEASTRACT: An upgraded database for the analysis of transcription regulatory networks in Saccharomyces cerevisiae. Nucleic Acids Res. 10.1093/nar/gkx842.

## STAR METHODS

## KEY RESOURCES TABLE

| REAGENT or RESOURCE | SOURCE | IDENTIFIER |
|---|---|---|
| **Chemicals** | | |
| Dimethyl sulfoxide | MP Biomedicals | Cat#196055; CAS: 67-68-5 |
| Rapamycin | Enzo | Cat#BML-A275-0025 |
| Antimycin A | Sigma | Cat#A8674; CAS: 1397-94-0 |
| Trichloroacetic Acid | Sigma | Cat#T6399; CAS: 7603-9 |
| PhosSTOP | Roche | Cat#04906837001 |
| cOmplete Protease Inhibitor Cocktail | Roche | Cat#11873580001 |
| HEPES | Sigma | Cat#H4034; CAS: 7365-45-9 |
| Magnesium Chloride | Kanto Chemical Co. Inc. | Cat#25009-00 |
| Sodium Chloride | 1st Base | Cat#BIO-1111-1KG |
| EDTA | Promega | Cat#V4233 |
| Triton X-100 | VWR | Cat#AAA16046-AP; CAS: 9002-93-1 |
| DL-Dithiothreitol (DTT) | Sigma | Cat#D9779; CAS: 3483-12-3 |
| Phenylmethanesulfonyl Fluoride (PMSF) | Sigma | Cat#36978; CAS: 329-98-6 |
| L-Leucine | Sigma | Cat#L8000; CAS: 61-90-5 |
| Uracil | Sigma | Cat#U0750; CAS: 66-22-8 |
| 2’,7’-Dichlorofluorescin diacetate | Sigma | Cat#D6883; CAS: 4091-99-0 |
| Dulbecco’s Modified Eagle Medium (DMEM), High Glucose | HyClone | Cat#SH30022.01 |

| | | |
|---|---|---|
| Fetal Bovine Serum, qualified, Brazil | Gibco | Cat#10270106 |
| Penicillin-Streptomycin (10,000U/mL) | Gibco | Cat#15140122 |
| **Critical Commercial Assays** | | |
| QuantiTect Reverse Transcriptase Kit | Qiagen | Cat#205313 |
| SYBR Fast Universal qPCR Kit, Kapa Biosystems | Sigma | Cat#KK4602 |
| RNeasy mini kit | Qiagen | Cat#74106 |
| PhosphoWorks™ Luminometric ATP Assay Kit | AAT Bioquest | Cat#21610 |
| Protein Assay Dye Reagent Concentrate | Bio-Rad | Cat#500-0006 |
| **Experimental Models: Organisms/Strains** | | |
| *S. cerevisiae* strain BY4743: genotype: WT | Euroscarf | N/A |
| *S. cerevisiae* BY4743 homozygous diploid deletion collection | Dharmacon | N/A |
| *S. cerevisiae* strain CEN.PK113-7D: genotype: WT | van Dijken et al. [66] | N/A |
| *S. cerevisiae* CEN.PK113-7D deletion strains | This paper | N/A |
| Human embryonic kidney cell line (HEK293) | ATCC | N/A |
| **Software and Algorithms** | | |
| ImageJ | NIH | https://imagej.nih.gov/ij/ |
| Prism | Graphpad software | https://www.graphpad.com/ |

## LEAD CONTACT AND MATERIALS AVAILABILITY

Further information and requests for resources and reagents should be directed to and will be fulfilled by the Lead Contact, Dr. Mohammad Alfatah (alfatahm@bii.a-star.edu.sg).

## EXPERIMENTAL MODEL AND SUBJECT DETAILS

### Yeast strains, growth media and cell culture

The *S. cerevisiae* auxotrophic BY4743 and prototrophic CEN.PK113-7D strains were used in this study. Deletion strains for BY4743 obtained from yeast homozygous diploid collection. Deletion strains in CEN.PK background was generated using standard PCR-based method [67]. Yeast strains were revived from frozen glycerol stock on YPD agar (1% Bacto yeast extract, 2% Bacto peptone, 2% glucose and 2.5% Bacto agar) medium for 2-3 days at 30°C.

### Human cell lines, growth media and cell culture

Human embryonic kidney cell line (HEK293) was cultured in high-glucose DMEM supplemented with 10% FBS and 1% Penicillin Streptomycin Solution. All cells cultured in a humidified incubator with 5% $CO_2$ at 37°C.

### Chemical treatment to cell culture

Stock solution of rapamycin and antimycin A was prepared in dimethyl sulfoxide (DMSO). The final concentration of DMSO did not exceed 1% in yeast and 0.01% in human cell lines experiments.

## METHOD DETAILS

### Data acquisition

The gene lists that modulate cellular lifespan in aging model organism *yeast Saccharomyces cerevisiae* were extracted from database SGD [19] and GenAge [20] (as of 8th November 2022). The actual gene lists are available in 'Additional File 1'.

### Yeast aging assay

For the chronological lifespan (CLS) experiments, prototrophic CEN.PK113-7D strains were grown in synthetic defined (SD) medium contain 6.7 g/L yeast nitrogen base with ammonium sulfate without amino acids and 2% glucose. SD medium supplemented with histidine (40

mg/L), leucine (160 mg/L), and uracil (40 mg/L) for auxotrophic BY4743 strains. Chronological aging was assessed by determining the lifespan of yeast as described previously with slight modifications [40]. Yeast culture grown in overnight at 30°C with 220 rpm shaking in glass flask was diluted to starting optical density at 600 nm ($OD_{600}$) ~ 0.2 in fresh medium to initiate the CLS experiment. CLS was performed by outgrowth method utilizing three different approaches: (i) Cells grown and aged in 96-well plates with a total 200 µL culture in SD medium at 30°C. At various age time points yeast stationary culture (2µL) were transferred to a second 96-well plate containing 200µL YPD medium and incubated for 24 hours at 30°C without shaking. Outgrowth $OD_{600}$ for each age point was measured by the microplate reader; (ii) Cells grown and aged in flask with a total culture volume more than 5 ml SD medium and incubated for 24 hours at 30°C with 220 rpm shaking. At different age time points yeast stationary culture washed and normalized to $OD_{600}$ of 1.0 with YPD medium. Further, normalized yeast cells were serial 10-fold diluted with YPD medium in 96-well plates. 3 µL of diluted culture were spotted onto the YPD agar plate and incubated for 48 hours at 30°C. The outgrowth of aged cells on the YPD agar plate was photographed using the GelDoc imaging system; (iii) The above discussed serial 10-fold diluted yeast stationary culture with YPD medium in 96-well plates incubated for 24 hours at 30°C without shaking. Outgrowth $OD_{600}$ for serial diluted aged cells was measured by the microplate reader.

**RNA extraction**

Yeast cells were first mechanically lysed using the manufacturer's disruption protocol. Total RNA from yeast cells was extracted using Qiagen RNeasy mini kit. ND-1000 UV-visible light spectrophotometer (Nanodrop Technologies) and Bioanalyzer 2100 with the RNA 6000 Nano Lab Chip kit (Agilent) was used to assess the concentration and integrity of RNA.

**RNA sequencing and bioinformatics analysis**

RNA sequencing (RNA-Seq) was conducted using NovaSeq PE150. Raw Fastq files were then passed into Fastp v0.23.2 for adapter trimming and low-quality reads removal. Both single end and paired end reads were processed with default parameters with --detect adapter for pe. Raw reads that passed the quality check were then aligned using HiSat 2 v2.2.1 with the index built from *Saccharomyces cerevisiae* R-64-1-1 top-level DNA fasta file obtained from Ensembl for sequencing data with S288C strain background. Library information for all experiments were first checked with RSeQC infer_experiment.py v4.0.0 before the addition of the respective parameters for alignment and counts. The resulting SAM files were then converted and sorted

to BAM files using Samtools v1.13. The BAM files were then used to generate feature counts using HTSeq v1.99.2. HTSeq counts from each experiment were then used for downstream Differentially Expressed Genes (DEG) analysis. Counts generated from HTSeq were then used for differential gene expression analysis using EdgeR v3.34.1 quasi likelihood F-test and DESeq2 v1.36.0. Principal Component Analysis (PCA) was conducted via the use of Transcript Per Million normalized counts. Samples that are separated by batches in the PCA were corrected using ComBat-Seq v3.44.0 before PCA was conducted after normalization of the corrected counts. Functional enrichment analysis was performed by metascape tool [28].

**qRT-PCR analysis**

Real time qRT-PCR experiments were performed as described previously using QuantiTect Reverse Transcription Kit (Qiagen) and SYBR Fast Universal qPCR Kit (Kapa Biosystems) [42]. The abundance of each gene was determined relative to the house-keeping transcript *ACT1*.

**ATP analysis**

Yeast cells were mixed with the final concentration of 5% trichloroacetic acid (TCA) and then kept on ice for at least 5 min. Cells were washed and resuspended in 10% TCA and lysis was performed with glass beads in a bead beater to extract the ATP. ATP extraction from human HEK293 cells was performed using Triton X-100 lysis buffer. The ATP level was quantified by PhosphoWorks™ Luminometric ATP Assay Kit (AAT Bioquest) and normalized by protein content measured Bio-Rad protein assay kit.

**ROS measurement**

Cells were washed and resuspended in 1× phosphate buffer saline (PBS, pH 7.4). After that cells were incubated with 40 μM H2DCFDA (Molecular probe) for 30 min at 30ºC. Cells were then washed with PBS and ROS level was measured by fluorescence reading (excitation at 485nm, emission at 524nm) by the microplate reader. The fluorescence intensity was normalized with $OD_{600}$.

**Transcription factors analysis**

Transcription factors (TFs) enrichment analysis was performed using YEASTRACT [68,69]. The significant p-value <0.05 considered for regulatory network analysis based on DNA-binding plus expression evidence. The TFs regulatory networks were visualized with a force-directed layout.

**Fermentative and respiratory growth assay**

Yeast cells grown in YPD medium were washed and normalized to $OD_{600}$ of 1.0 with water. Further, normalized yeast cells were serial 10-fold diluted with water. 3 µL of diluted culture were spotted onto the agar medium YPD (2% glucose) and YPG (3% glycerol) and incubated for 48 hours at 30ºC. The cell growth on the agar plate was photographed using the GelDoc imaging system.

**Growth sensitivity assay**

Effect of chemical compounds on cell growth was carried out in 96-well plates. At an $OD_{600}$ of ~ 0.2 in SD medium 200 µL yeast cells was transferred into the 96-well plate containing serially double-diluted concentrations of compounds. Cells were incubated at 30°C and the growth was measured at $OD_{600}$ by the microplate reader.

## QUANTIFICATION AND STATISTICAL ANALYSIS

Data analysis of all the experimental results such as mean value, standard deviations, significance, and graphing were performed using GraphPad Prism v.9.3.1 software. The comparison of obtained results were statistically performed using the Student's t-tests, Ordinary One-way ANOVA and Two-way ANOVA followed by multiples comparison tests. In all the graph plots, P values are shown as *P < 0.05, **P < 0.01, ***P < 0.001, and ****P < 0.0001 were considered significant. ns: non-significant.

## DATA AVAILABILITY

https://data.mendeley.com/datasets/bj84wx7tf4/draft?a=dd92d261-94bd-4220-811a-81a9d761c857

## SUPPLEMENTARY FIGURE LEGEND

**Figure S1. Transcriptomics analysis of rapamycin to identify the TORC1 regulated genes**
(A and B) Chronological lifespan (CLS) of the wild type BY4743 (A) and CEN.PK113-7D (B) yeast strains was assessed in the SD medium supplemented with auxotrophic amino acids (A) and only the SD medium (B) in 96-well plate. Aged cells survival was measured relative to the outgrowth of day 2. Data are represented as means ± SD (n=4). *P < 0.05, and ****P < 0.0001 based on two-way ANOVA followed by Dunnett's multiple comparisons test. ns: non-significant.

(C) Principal component analysis (PCA) of the RNA-seq data from replicates of DMSO and rapamycin (50 nM) treated yeast cells (BY4743). PC1 represents 95.98% of the total variance in the experimental data, and PC2 represents 2.59% of the total variance.

(D and E) Volcano plots produced by EdgeR (D) and DESeq2 (E) demonstrate the gene expression pattern and the differentially expressed genes (DEGs) with p-value <0.05, with a fold change of $\log_2$(fold change) >1 for upregulated genes and $\log_2$(fold change) <−1 for downregulated genes.

(F) Overlap of identified DEGs using EdgeR and DESeq2 with the criteria for all two tools that p-value <0.05, with a fold change of $\log_2$(fold change) >1 for upregulated genes and $\log_2$(fold change) <−1 for downregulated genes. Upregulated and downregulated DEGs overlaps for both EdgeR and DESeq2 were further considered for functional GO enrichment analysis.

See also Additional File 2.

**Figure S2. RNA sequencing data validation by qRT-PCR**
(A and B) Expression analysis of selected genes of RNA sequencing (RNA-seq) data by qRT-PCR in in *Saccharomyces cerevisiae* genetic backgrounds BY4743 (A) and CEN.PK113-7D (B) wild type cells treated with DMSO and rapamycin (50 nM). Gene expression of rapamycin treated samples were compared with DMSO control. Data are represented as means ± SD (n=4). *P < 0.05, **P < 0.01, ***P < 0.001, and ****P < 0.0001 based on two-sided Student's t-tests.

**Figure S3. Identification of the role of uncharacterized *YBR238C* gene in cellular aging, Related to Figure 2**

(A) Principal component analysis (PCA) of the RNA-seq data from replicates of wild type BY4743 and ybr*238c*Δ yeast strains. PC1 represents 71.75% of the total variance in the experimental data, and PC2 represents 18.15% of the total variance.

(B) Volcano plots produced by DESeq2 demonstrate the gene expression pattern and the differentially expressed genes (DEGs) with p-value <0.05, with a fold change of $\log_2$(fold change) >0.5 for upregulated genes and $\log_2$(fold change) <−0.5 for downregulated genes. GO enrichment analysis was performed for upregulated DEGs. See also Additional File 3.

(C and D) Comparison of functional enrichment analysis for upregulated DEGs of *ybr238c*Δ mutant and rapamycin (50 nM) treated wild type BY4743 cells. Bar plots showing the common enriched biological process (C) and MCODE complexes based on the top-three ontology enriched terms (D).

**Figure S4. Transcription factors analysis for upregulated DEGs of *ybr238c*Δ mutant, Related to Figure 2**

(A) The whole regulatory network of overrepresented top eight enriched transcription factors (blue) within the upregulated DEGs of *ybr238c*Δ mutant. Msn4 and Hap4 TFs are appearing as responsible for the highest number of regulated genes in *ybr238c*Δ mutant.

(B) The Msn4 regulon within the upregulated DEGs of *ybr238c*Δ mutant.

See also Additional File 3.

**Figure S5. *YBR238C* homolog *RMD9* deletion leads to mitochondrial dysfunction associated with accelerated cellular aging, Related to Figure 4**

(A and E) Chronological lifespan (CLS) of yeast wild type BY4743 and deletion strains was performed in the SD medium supplemented with auxotrophic amino acids in 96-well plate. Aged cells survival was measured relative to the outgrowth of day 1. (A) Data are represented

as means ± SD (n=12). ****P < 0.0001 based on two-way ANOVA followed by Tukey's multiple comparisons test. (E) Data are represented as means ± SD (n=4). ****P < 0.0001 based on ordinary one-way ANOVA followed by Dunnett's multiple comparisons test. ns: non-significant.

(B, C, F and G) CLS of yeast wild type BY4743 and deletion strains was performed in the flask. Outgrowth was performed for ten-fold serial diluted aged cells onto the YPD agar plate (B and F) and YPD medium in the 96-well plate (C and G). The serial outgrowth of aged cells on agar medium was imaged (B and F) and quantified the survival relative to outgrowth of day 1 (C and G). A representative of two experiments for B, C, F and G is shown.

(D) Serial dilution growth assays of the yeast strains on fermentative glucose medium (YPD) and respiratory glycerol medium (YPG).

(H) ROS level of yeast wild type BY4743 and deletion strains. Data are represented as means ± SD (n=3). **P < 0.01, and ****P < 0.0001 based on ordinary one-way ANOVA followed by Dunnett's multiple comparisons test.

**Figure S6. TORC1-Mitochondrial function signaling pathways control cellular aging**

(A and C) ATP analysis of wild type CEN.PK113-7D yeast cells treated with (A) antimycin A (stationary phase culture) and (C) rapamycin (logarithmic phase culture). Data are represented as means ± SD (n=3). ***P < 0.001, and ****P < 0.0001 based on ordinary one-way ANOVA followed by Dunnett's multiple comparisons test.

(B) Chronological lifespan (CLS) of wild type yeast strain with indicated concentrations of antimycin A was performed in the SD medium in 96-well plate. Aged cells survival was measured relative to the outgrowth of day 1. Data are represented as means ± SD (n=8). ***P < 0.001, and ****P < 0.0001 based on two-way ANOVA followed by Dunnett's multiple comparisons test. ns: non-significant. ns: non-significant.

(D and E) Expression analysis by qRT-PCR for *YBR238C* in logarithmic phase yeast strains treated with rapamycin (200 nM) for 1 hour. Data are represented as means ± SD (n=2). **P < 0.01, and ****P < 0.0001 based on two-sided Student’s t-test.

(F) CLS of yeast strains with indicated concentrations of rapamycin was performed in the SD medium in 96-well plate. Aged cells survival was measured relative to the outgrowth of day 2. Data are represented as means ± SD (n=3). ****P < 0.0001 based on two-way ANOVA followed by Dunnett's multiple comparisons test. ns: non-significant. See also Figure 6D.

(G) Growth assay of yeast strains with rapamycin (40 nM) for 24 and 48h. Growth was normalized with untreated control.

(H) Growth assay of yeast strains with indicated concentrations of rapamycin for 48, 72 and 96 h. Growth was normalized with untreated control.

(I) ATP analysis of stationary phase wild type CEN.PK113-7D yeast cells were incubated with indicated concentrations of rapamycin. Data are represented as means ± SD (n=6). ****P < 0.0001 based on ordinary one-way ANOVA followed by Tukey's multiple comparisons test.

(J) ATP analysis of human HEK293 cells treated with antimycin A (10 µM) and rapamycin (100 nM) for 48 hours. Data are represented as means ± SD (n=3). ****P < 0.0001 based on ordinary one-way ANOVA followed by Tukey's multiple comparisons test.

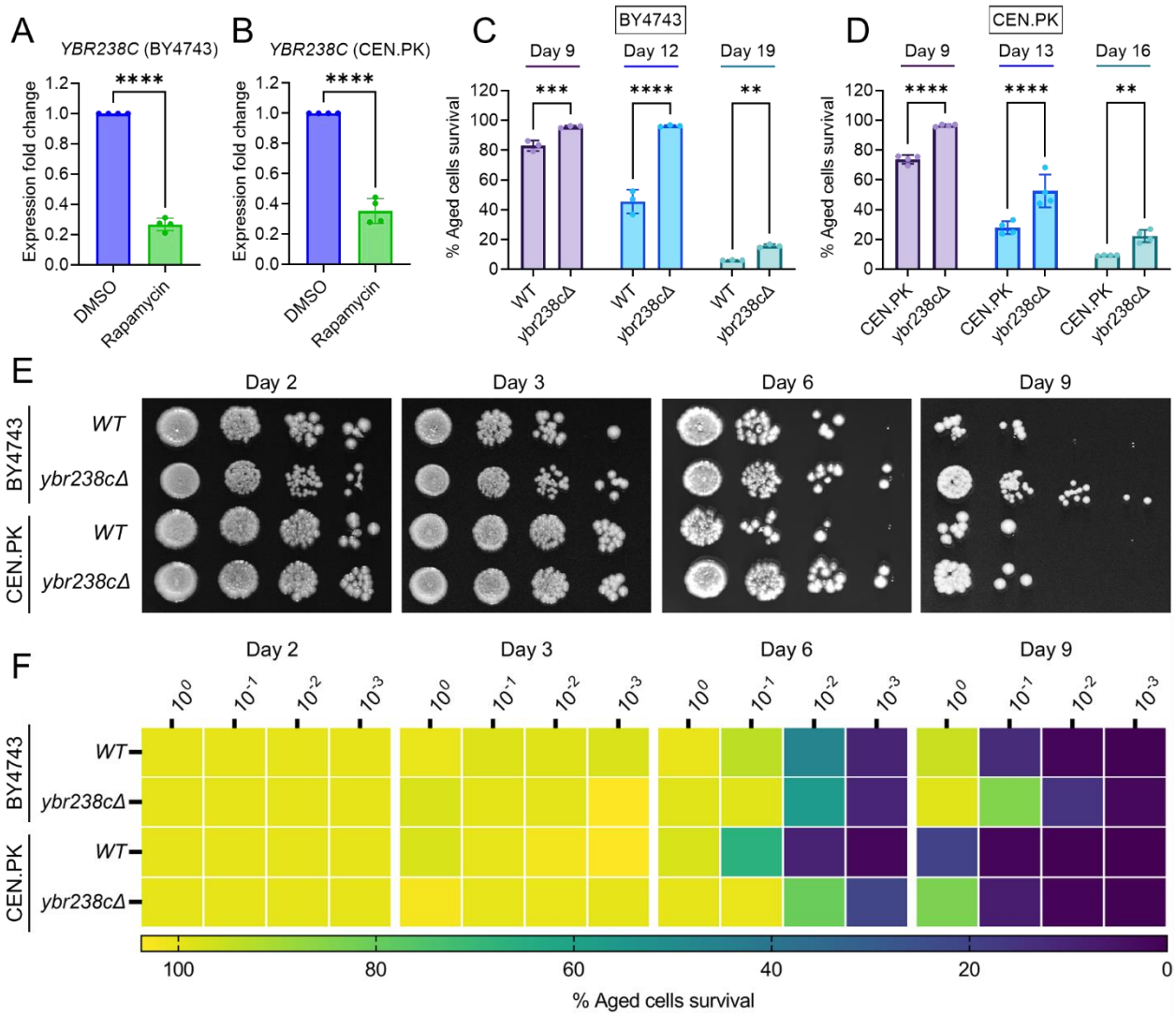
A
YBR238C (BY4743)
Expression fold change
****
DMSO
Rapamycin
B
YBR238C (CEN.PK)
C
BY4743
Day 9
Day 12
Day 19
% Aged cells survival
***
****
**
WT
ybr238cΔ
D
CEN.PK
Day 13
Day 16
E
Day 2
Day 3
Day 6
Day 9
BY4743
CEN.PK
F
% Aged cells survival

**Figure 1**

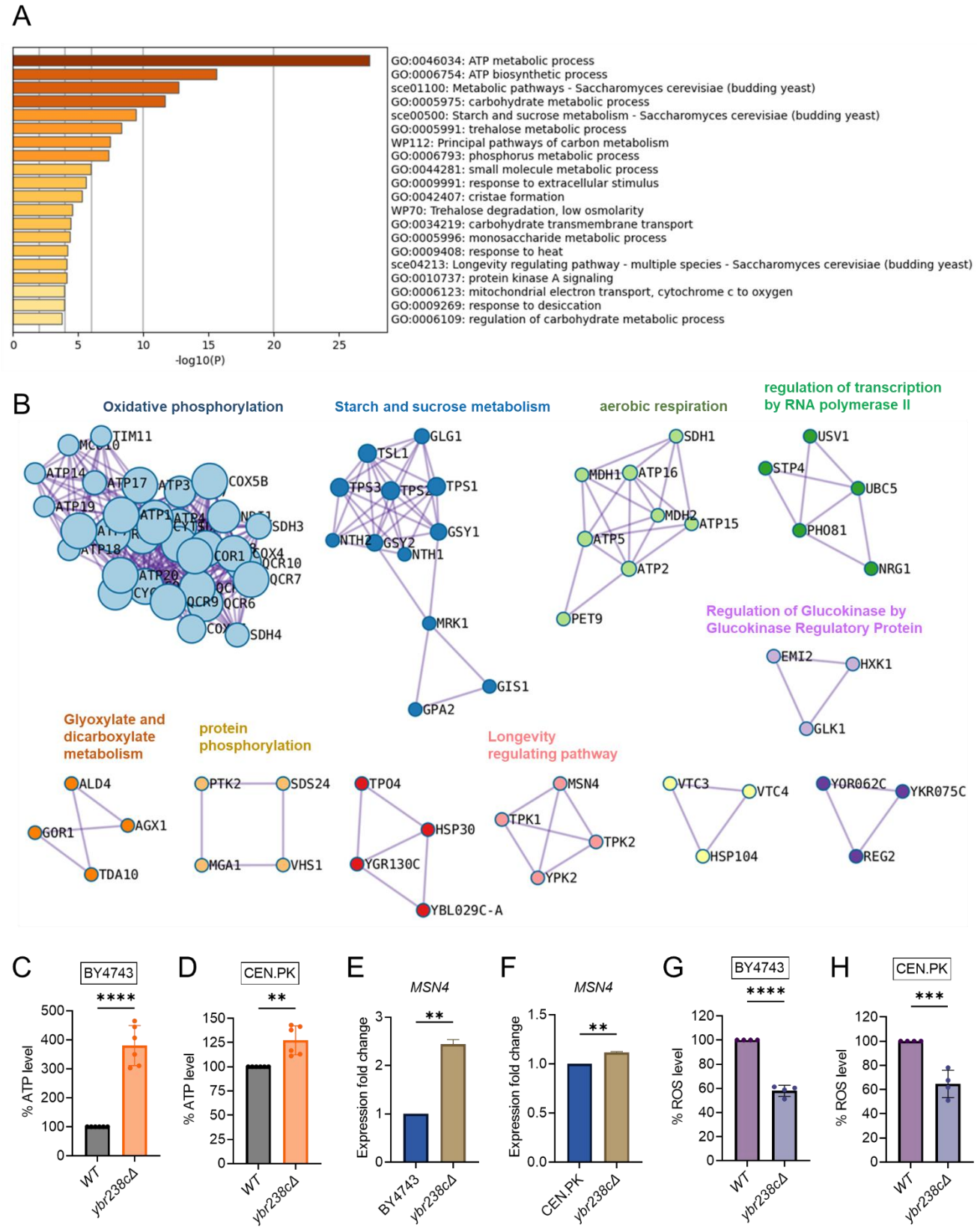
A
GO:0046034: ATP metabolic process
GO:0006754: ATP biosynthetic process
sce01100: Metabolic pathways - Saccharomyces cerevisiae (budding yeast)
GO:0005975: carbohydrate metabolic process
sce00500: Starch and sucrose metabolism - Saccharomyces cerevisiae (budding yeast)
GO:0005991: trehalose metabolic process
WP112: Principal pathways of carbon metabolism
GO:0006793: phosphorus metabolic process
GO:0044281: small molecule metabolic process
GO:0009991: response to extracellular stimulus
GO:0042407: cristae formation
WP70: Trehalose degradation, low osmolarity
GO:0034219: carbohydrate transmembrane transport
GO:0005996: monosaccharide metabolic process
GO:0009408: response to heat
sce04213: Longevity regulating pathway - multiple species - Saccharomyces cerevisiae (budding yeast)
GO:0010737: protein kinase A signaling
GO:0006123: mitochondrial electron transport, cytochrome c to oxygen
GO:0009269: response to desiccation
GO:0006109: regulation of carbohydrate metabolic process
-log10(P)
B
Oxidative phosphorylation
Starch and sucrose metabolism
aerobic respiration
regulation of transcription by RNA polymerase II
Regulation of Glucokinase by Glucokinase Regulatory Protein
Glyoxylate and dicarboxylate metabolism
protein phosphorylation
Longevity regulating pathway
C
BY4743
% ATP level
WT
ybr238cΔ
D
CEN.PK
% ATP level
E
MSN4
Expression fold change
F
MSN4
Expression fold change
G
BY4743
% ROS level
H
CEN.PK
% ROS level

**Figure 2**

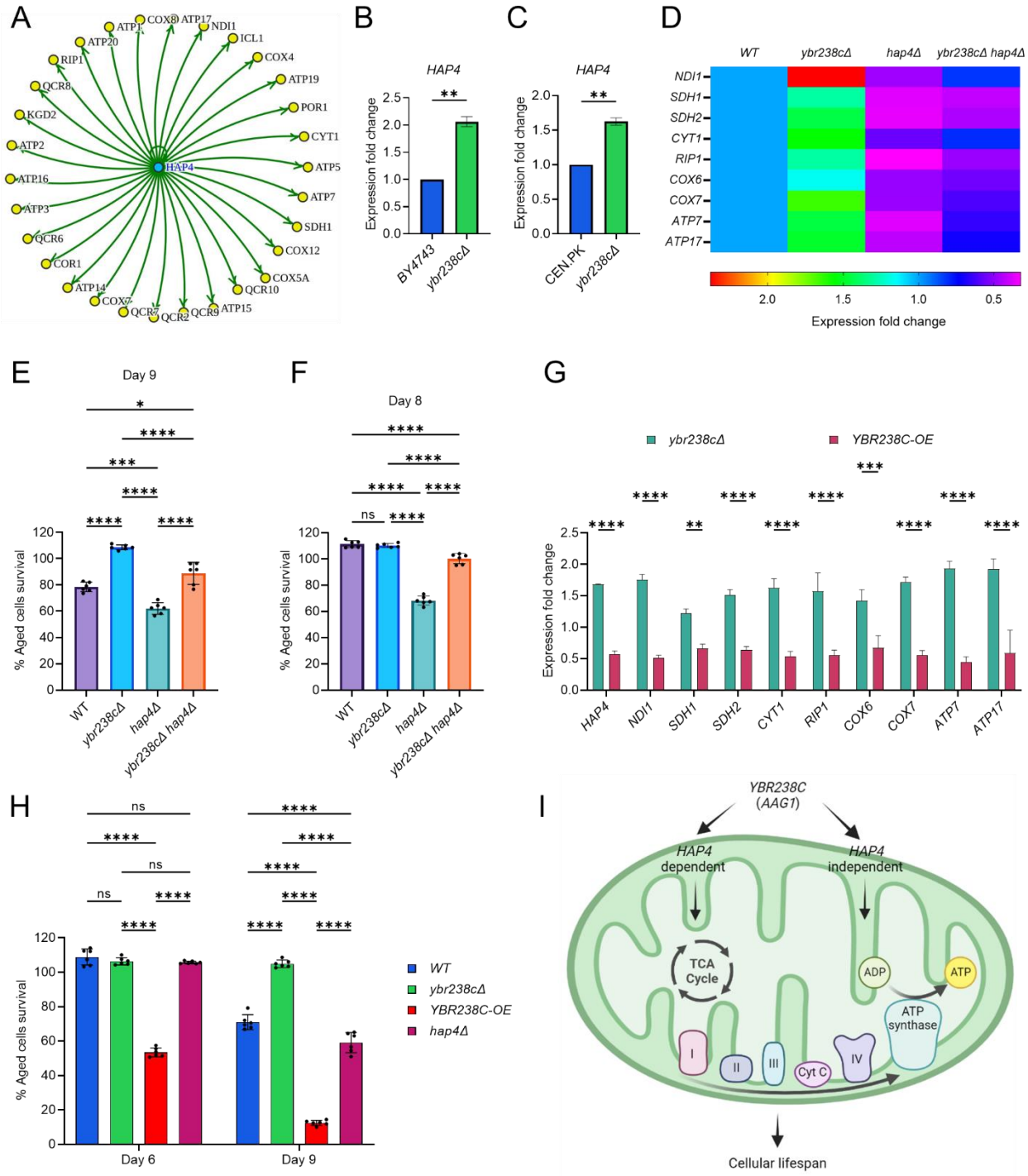
A
HAP4
COX8
ATP17
NDI1
ICL1
COX4
ATP19
POR1
CYT1
ATP5
ATP7
SDH1
COX12
COX5A
QCR10
ATP15
QCR9
QCR2
QCR7
COX7
ATP14
COR1
QCR6
ATP3
ATP16
ATP2
KGD2
QCR8
RIP1
ATP20
ATP1
B
HAP4
Expression fold change
BY4743
ybr238cΔ
C
HAP4
Expression fold change
CEN.PK
ybr238cΔ
D
WT
ybr238cΔ
hap4Δ
ybr238cΔ hap4Δ
NDI1
SDH1
SDH2
CYT1
RIP1
COX6
COX7
ATP7
ATP17
Expression fold change
E
Day 9
% Aged cells survival
WT
ybr238cΔ
hap4Δ
ybr238cΔ hap4Δ
F
Day 8
% Aged cells survival
G
ybr238cΔ
YBR238C-OE
Expression fold change
HAP4
NDI1
SDH1
SDH2
CYT1
RIP1
COX6
COX7
ATP7
ATP17
H
% Aged cells survival
Day 6
Day 9
WT
ybr238cΔ
YBR238C-OE
hap4Δ
I
YBR238C
(AAG1)
HAP4
dependent
HAP4
independent
TCA
Cycle
ADP
ATP
ATP
synthase
I
II
III
Cyt C
IV
Cellular lifespan

**Figure 3**

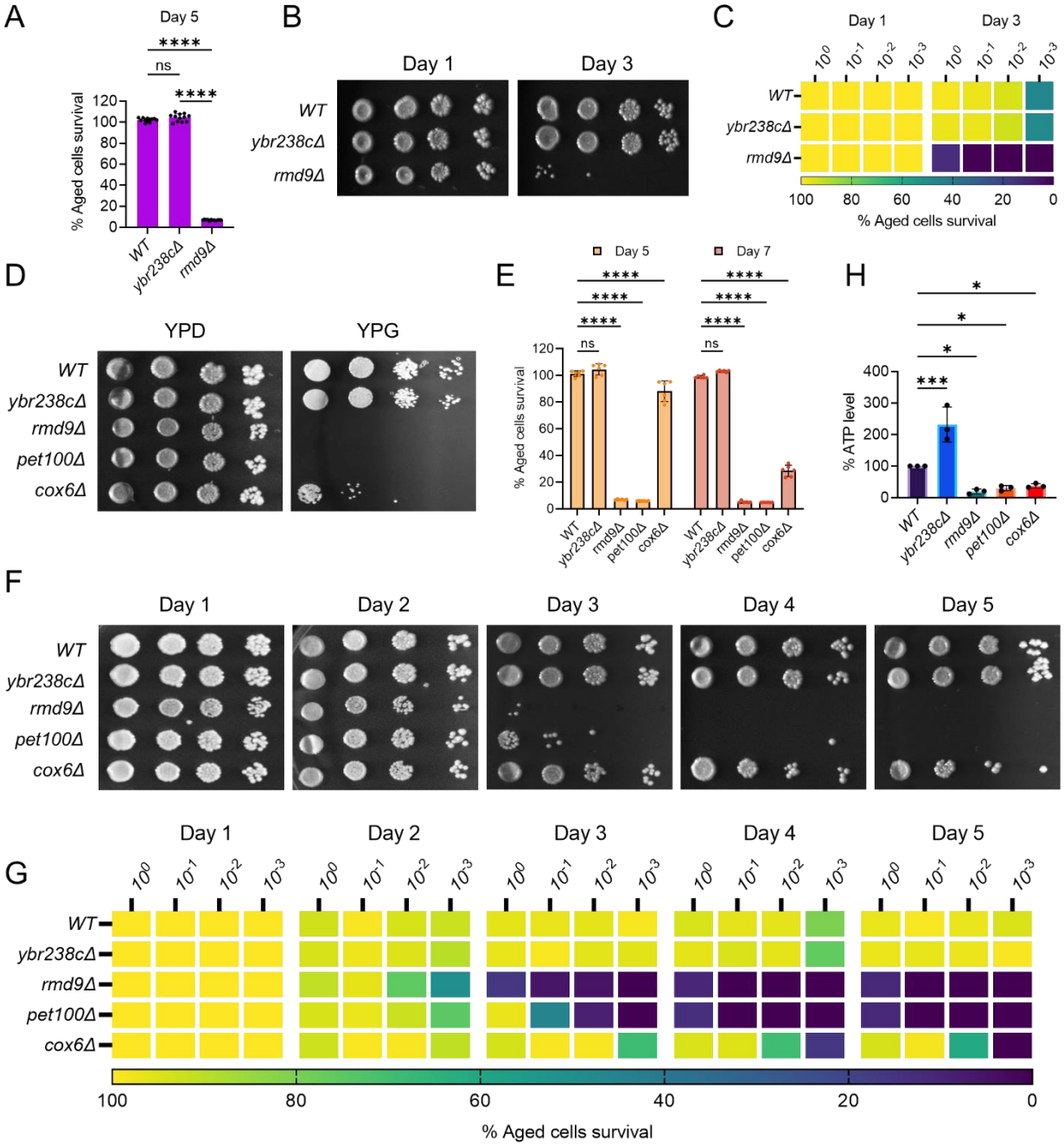
A
Day 5
****
ns
****
% Aged cells survival
120
100
80
60
40
20
0
WT
ybr238cΔ
rmd9Δ
B
Day 1
Day 3
WT
ybr238cΔ
rmd9Δ
C
Day 1
Day 3
10^0
10^-1
10^-2
10^-3
WT
ybr238cΔ
rmd9Δ
100
80
60
40
20
0
% Aged cells survival
D
YPD
YPG
WT
ybr238cΔ
rmd9Δ
pet100Δ
cox6Δ
E
Day 5
Day 7
****
ns
% Aged cells survival
WT
ybr238cΔ
rmd9Δ
pet100Δ
cox6Δ
H
*
***
% ATP level
400
300
200
100
0
WT
ybr238cΔ
rmd9Δ
pet100Δ
cox6Δ
F
Day 1
Day 2
Day 3
Day 4
Day 5
WT
ybr238cΔ
rmd9Δ
pet100Δ
cox6Δ
G
Day 1
Day 2
Day 3
Day 4
Day 5
10^0
10^-1
10^-2
10^-3
WT
ybr238cΔ
rmd9Δ
pet100Δ
cox6Δ
100
80
60
40
20
0
% Aged cells survival

**Figure 4**

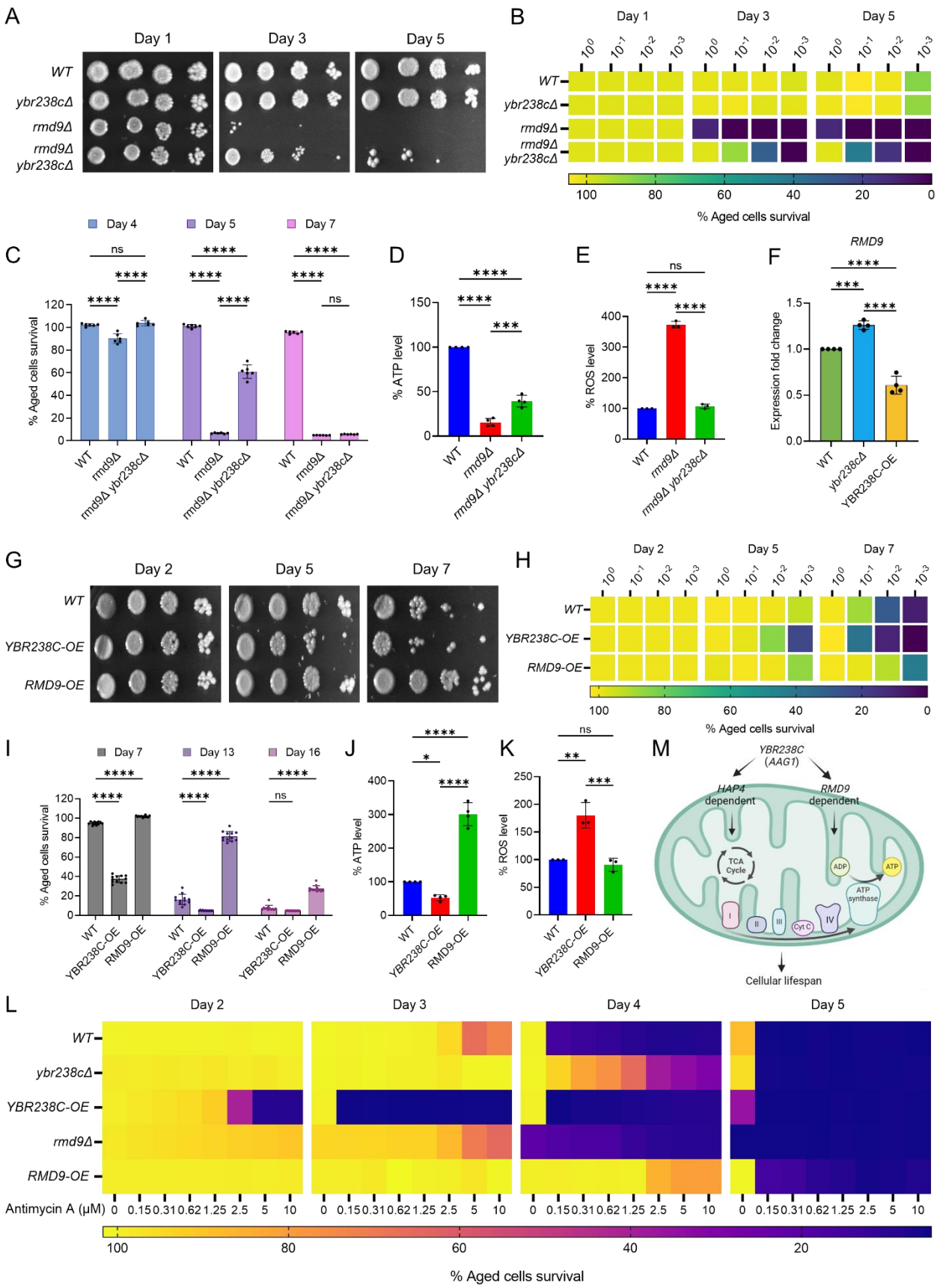
A
Day 1
Day 3
Day 5
WT
ybr238cΔ
rmd9Δ
rmd9Δ ybr238cΔ
B
Day 1
Day 3
Day 5
% Aged cells survival
C
Day 4
Day 5
Day 7
% Aged cells survival
D
% ATP level
E
% ROS level
F
RMD9
Expression fold change
G
Day 2
Day 5
Day 7
YBR238C-OE
RMD9-OE
H
I
Day 7
Day 13
Day 16
J
K
M
YBR238C (AAG1)
HAP4 dependent
RMD9 dependent
TCA Cycle
ATP synthase
Cellular lifespan
L
Antimycin A (μM)

**Figure 5**

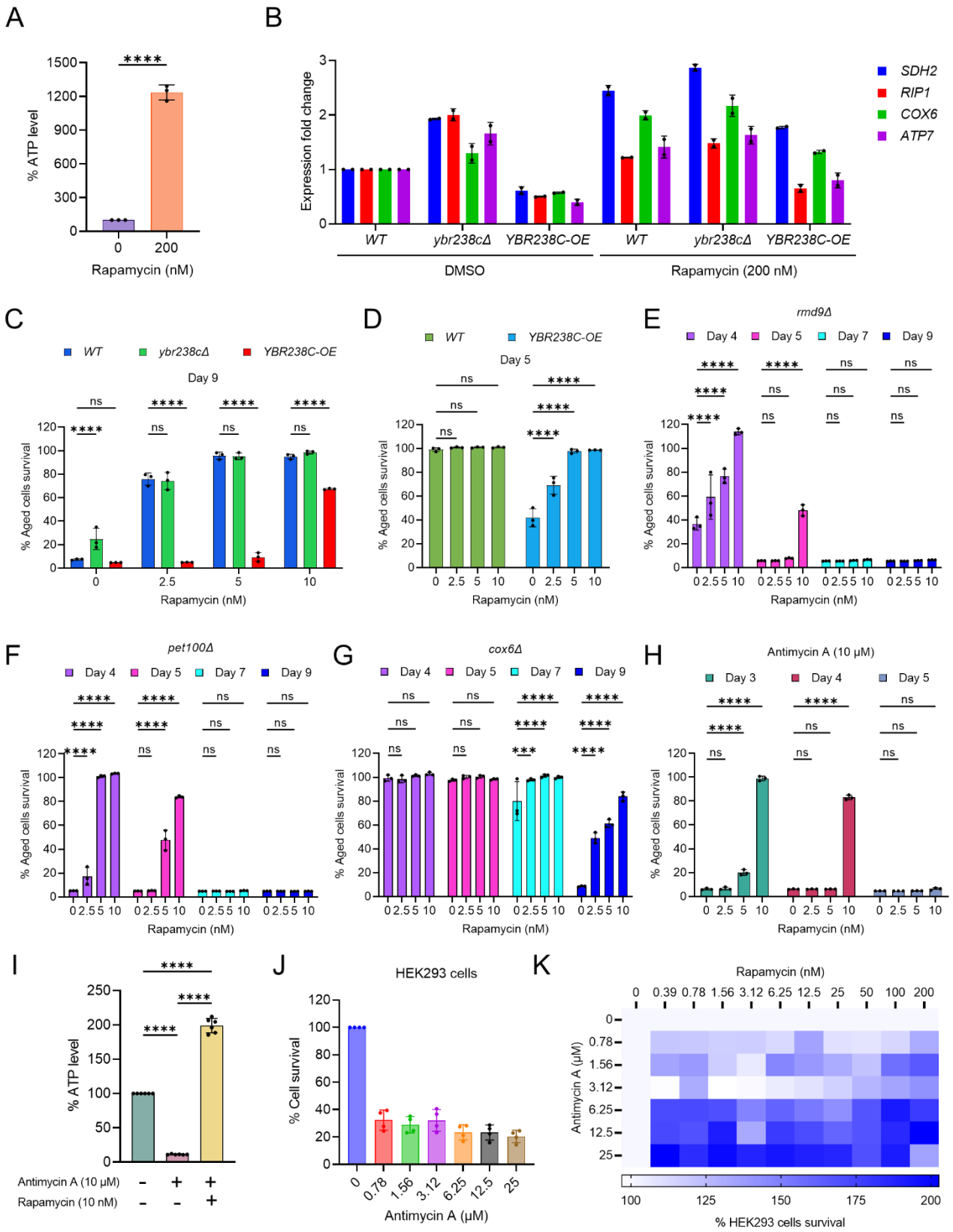
A
% ATP level
Rapamycin (nM)
B
Expression fold change
SDH2
RIP1
COX6
ATP7
WT
ybr238cΔ
YBR238C-OE
DMSO
Rapamycin (200 nM)
C
Day 9
% Aged cells survival
Rapamycin (nM)
D
Day 5
E
rmd9Δ
Day 4
Day 5
Day 7
Day 9
F
pet100Δ
G
cox6Δ
H
Antimycin A (10 μM)
Day 3
I
% ATP level
Antimycin A (10 μM)
Rapamycin (10 nM)
J
HEK293 cells
% Cell survival
Antimycin A (μM)
K
Rapamycin (nM)
Antimycin A (μM)
% HEK293 cells survival

**Figure 6**

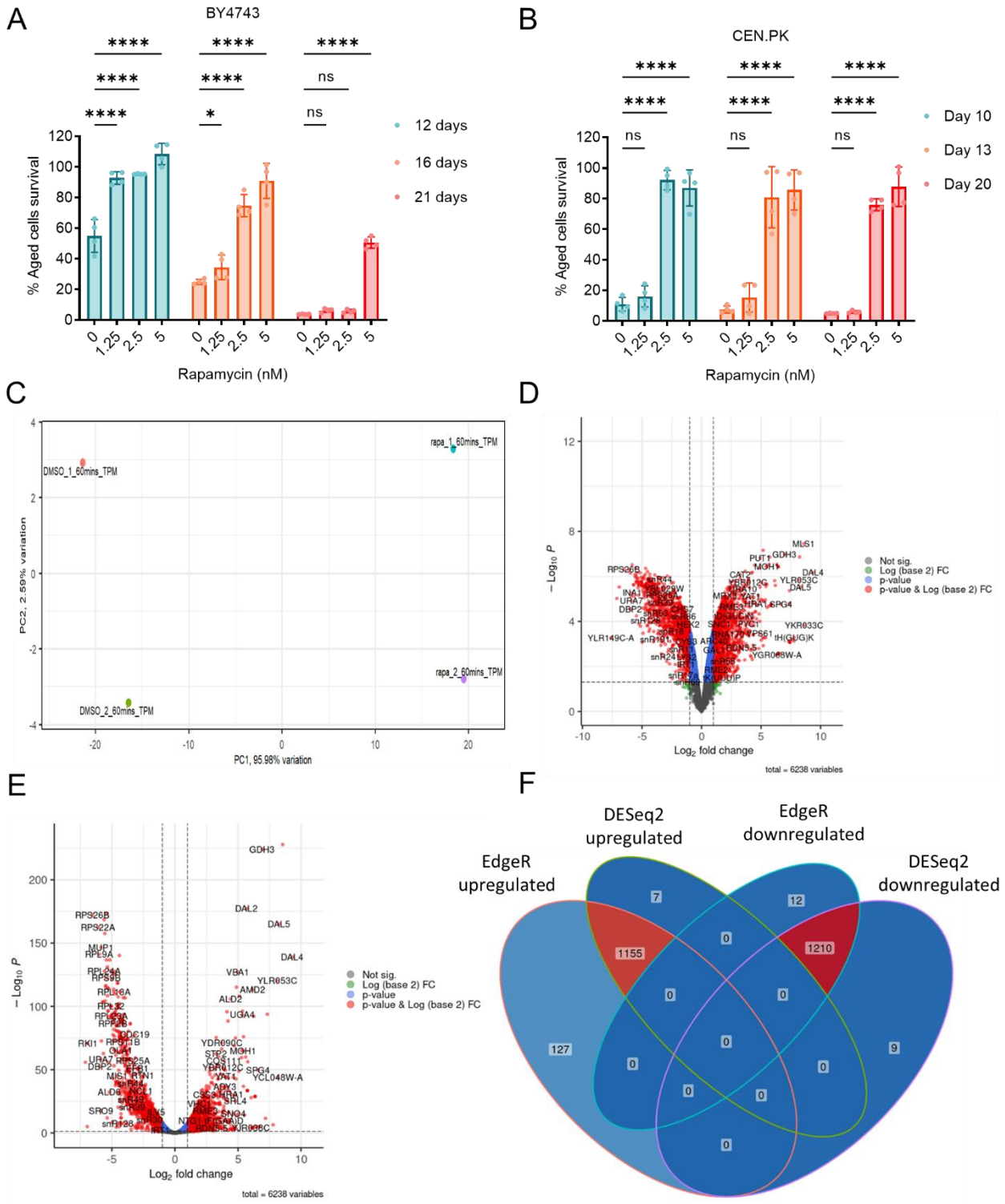
A
BY4743
% Aged cells survival
Rapamycin (nM)
12 days
16 days
21 days
B
CEN.PK
Day 10
Day 13
Day 20
C
PC2, 2.59% variation
PC1, 95.98% variation
rapa_1_60mins_TPM
DMSO_1_60mins_TPM
rapa_2_60mins_TPM
DMSO_2_60mins_TPM
D
Not sig.
Log (base 2) FC
p-value
p-value & Log (base 2) FC
Log2 fold change
total = 6238 variables
E
F
DESeq2 upregulated
EdgeR downregulated
EdgeR upregulated
DESeq2 downregulated

**Figure S1**

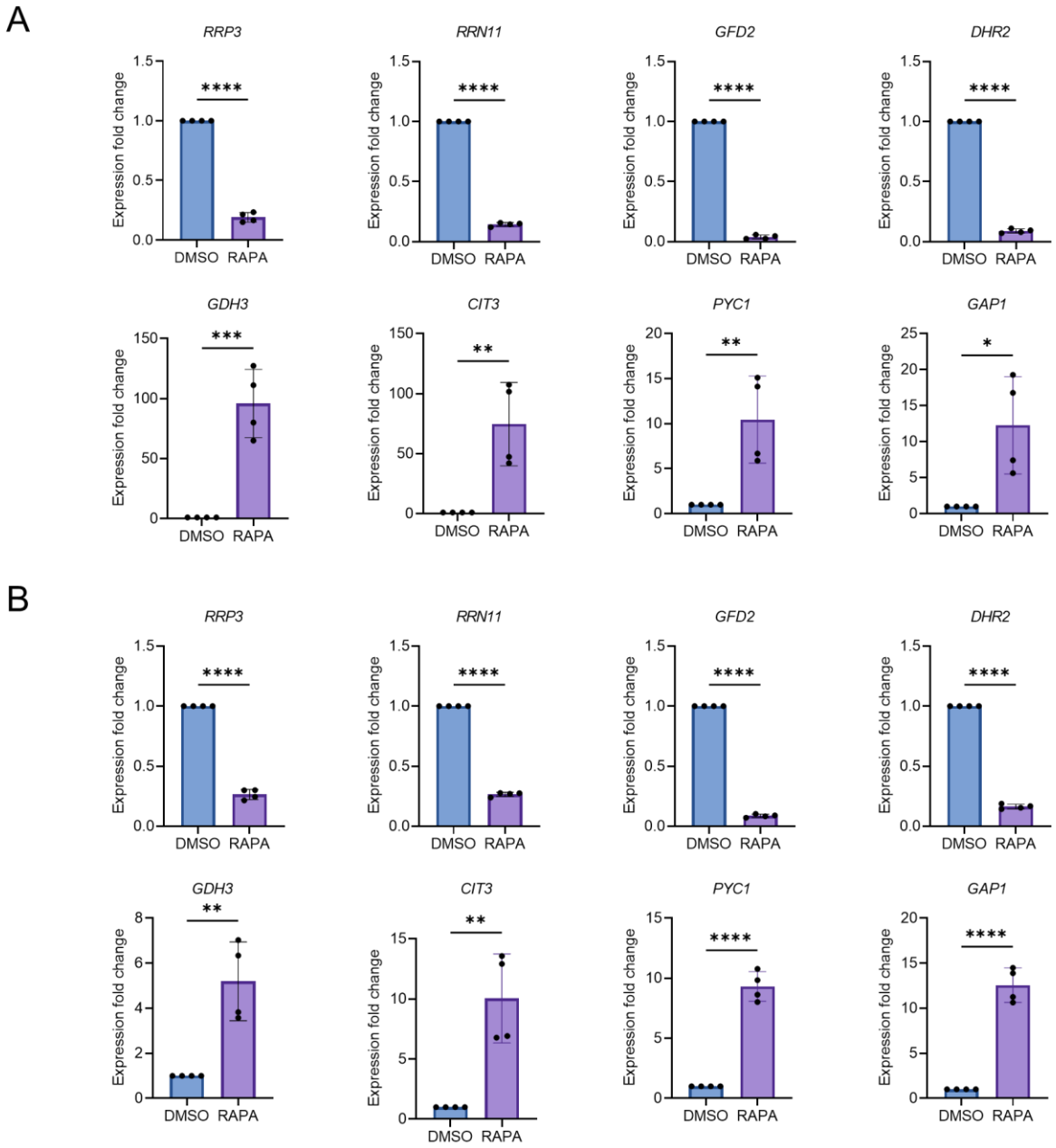
A
RRP3
RRN11
GFD2
DHR2
GDH3
CIT3
PYC1
GAP1
Expression fold change
DMSO
RAPA
****
***
**
*
B

**Figure S2**

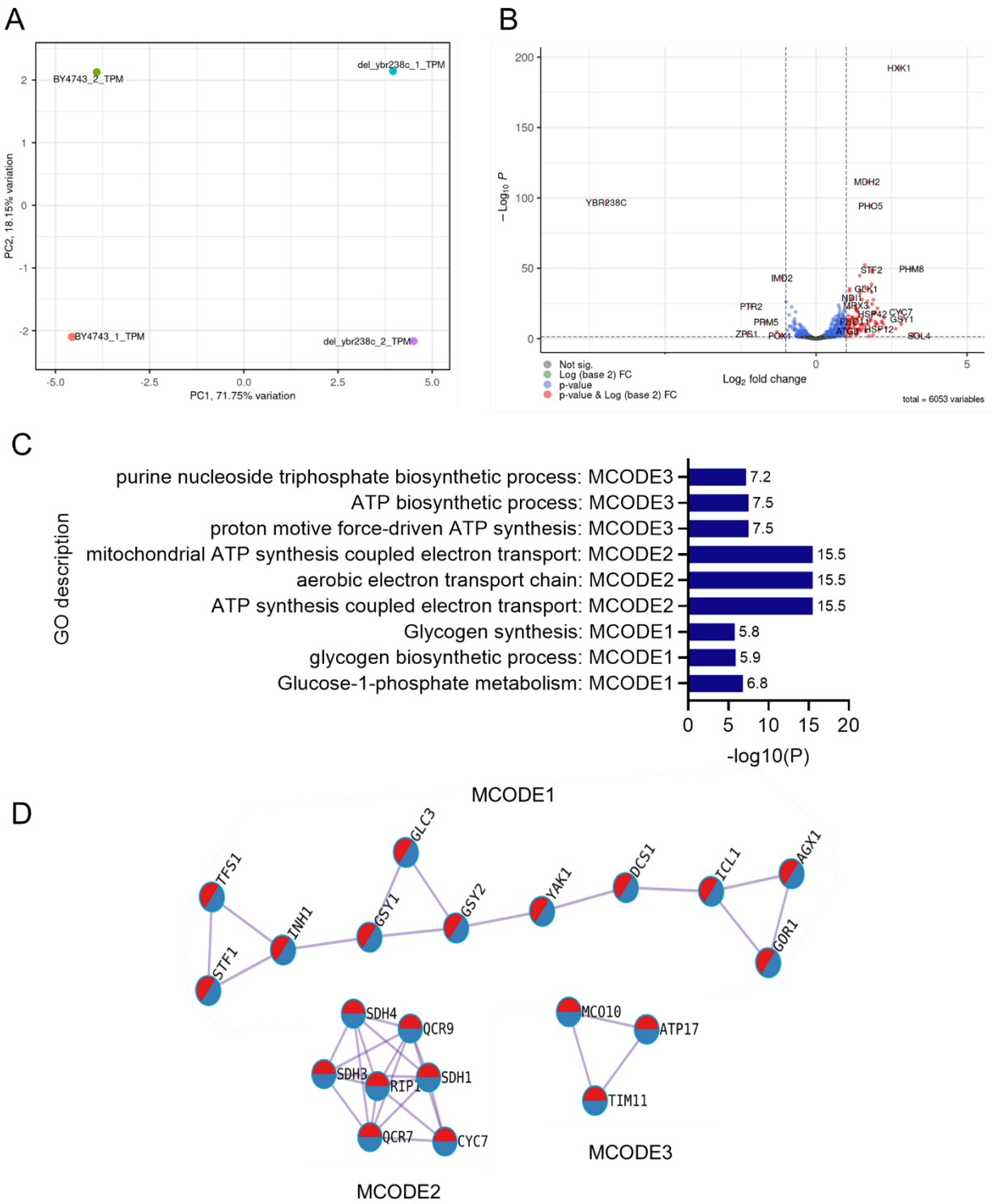
A
BY4743_2_TPM
del_ybr238c_1_TPM
BY4743_1_TPM
del_ybr238c_2_TPM
PC2, 18.15% variation
PC1, 71.75% variation
B
HXK1
MDH2
PHO5
YBR238C
STF2
PHM8
IMD2
GCK1
NDI1
MRX3
HSP42
CYC7
GSY1
PTR2
PRM5
ZRS1
POX1
ATG8
HSP12
SOL4
Not sig.
Log (base 2) FC
p-value
p-value & Log (base 2) FC
Log2 fold change
total = 6053 variables
C
GO description
purine nucleoside triphosphate biosynthetic process: MCODE3
ATP biosynthetic process: MCODE3
proton motive force-driven ATP synthesis: MCODE3
mitochondrial ATP synthesis coupled electron transport: MCODE2
aerobic electron transport chain: MCODE2
ATP synthesis coupled electron transport: MCODE2
Glycogen synthesis: MCODE1
glycogen biosynthetic process: MCODE1
Glucose-1-phosphate metabolism: MCODE1
7.2
7.5
7.5
15.5
15.5
15.5
5.8
5.9
6.8
-log10(P)
D
MCODE1
TFS1
GLC3
INH1
GSY1
GSY2
YAK1
DCS1
ICL1
AGX1
STF1
GOR1
SDH4
QCR9
SDH3
RIP1
SDH1
QCR7
CYC7
MCO10
ATP17
TIM11
MCODE3
MCODE2

**Figure S3**

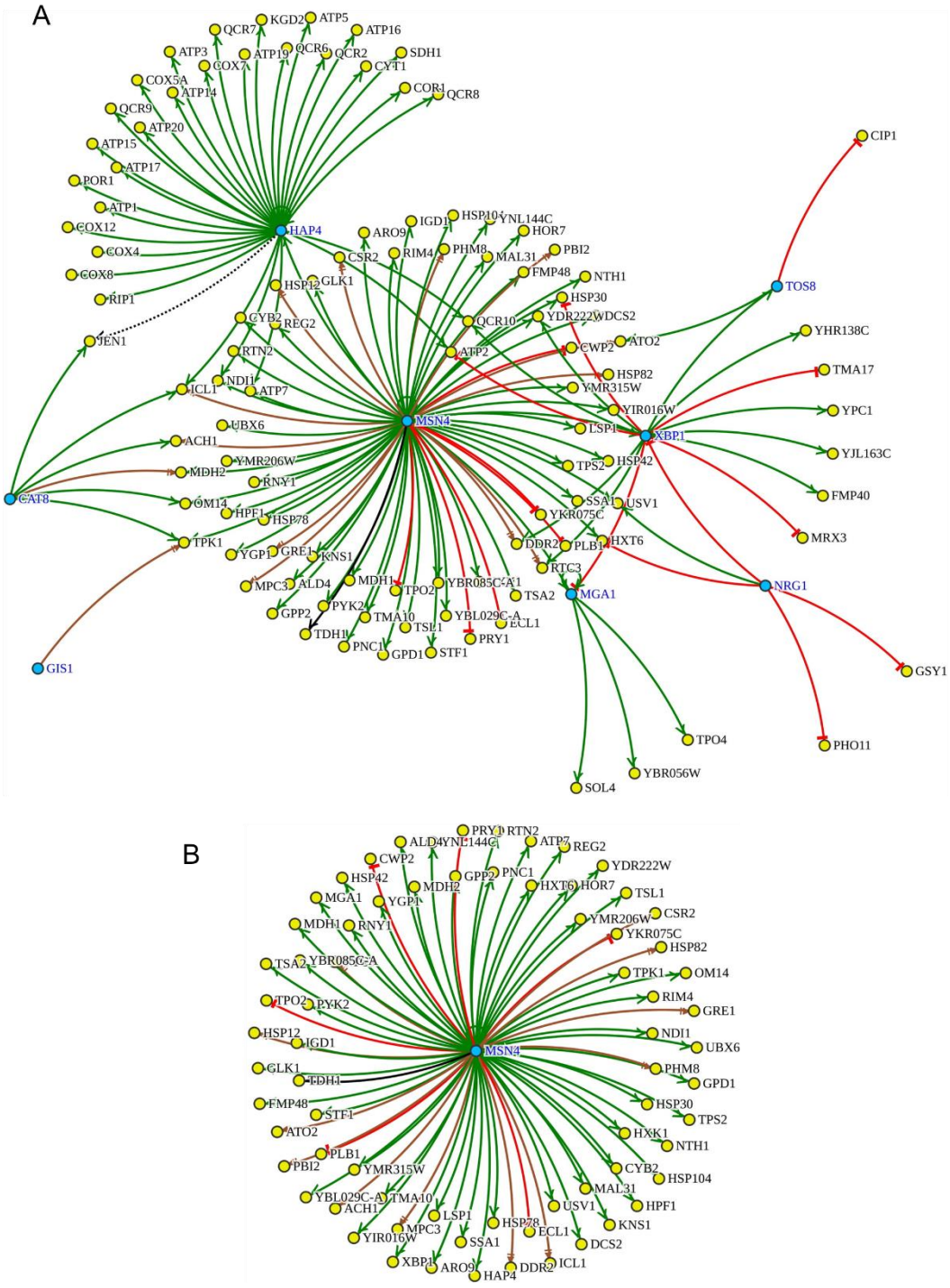
A
QCR7
KGD2
ATP5
ATP16
ATP3
ATP19
QCR6
QCR2
SDH1
COX7
CYT1
COX5A
ATP14
COR1
QCR8
QCR9
ATP20
ATP15
ATP17
POR1
ATP1
COX12
HAP4
IGD1
HSP10
YNL144C
HOR7
ARO9
COX4
CSR2
RIM4
PHM8
MAL31
PBI2
COX8
FMP48
NTH1
HSP12
GLK1
HSP30
RIP1
CYB2
REG2
QCR10
YDR222W
DCS2
JEN1
RTN2
ATP2
CWP2
ATO2
NDI1
HSP82
ICL1
ATP7
YMR315W
MSN4
YIR016W
UBX6
LSP1
XBP1
ACH1
YMR206W
TPS2
HSP42
MDH2
RNY1
SSA1
USV1
CAT8
OM14
HPF1
HSP78
YKR075C
TPK1
DDR2
PLB1
HXT6
YGP1
GRE1
KNS1
RTC3
MPC3
ALD4
MDH1
TPO2
YBR085C-A
TSA2
MGA1
GPP2
PYK2
TMA10
YBL029C-A
ECL1
TDH1
TSL1
PRY1
PNC1
GPD1
STF1
GIS1
CIP1
TOS8
YHR138C
TMA17
YPC1
YJL163C
FMP40
MRX3
NRG1
GSY1
PHO11
TPO4
YBR056W
SOL4
B
PRY1
RTN2
ALD4
YNL144C
ATP7
REG2
CWP2
YDR222W
HSP42
GPP2
PNC1
MDH2
HXT6
HOR7
MGA1
YGP1
TSL1
CSR2
MDH1
RNY1
YMR206W
YKR075C
HSP82
TSA2
YBR085C-A
TPK1
OM14
TPO2
PYK2
RIM4
GRE1
HSP12
IGD1
NDI1
UBX6
MSN4
GLK1
TDH1
PHM8
GPD1
FMP48
HSP30
STF1
TPS2
ATO2
HXK1
NTH1
PLB1
PBI2
YMR315W
CYB2
HSP104
YBL029C-A
TMA10
MAL31
ACH1
USV1
HPF1
LSP1
HSP78
KNS1
MPC3
ECL1
YIR016W
SSA1
DCS2
XBP1
ARO9
DDR2
ICL1
HAP4

**Figure S4**

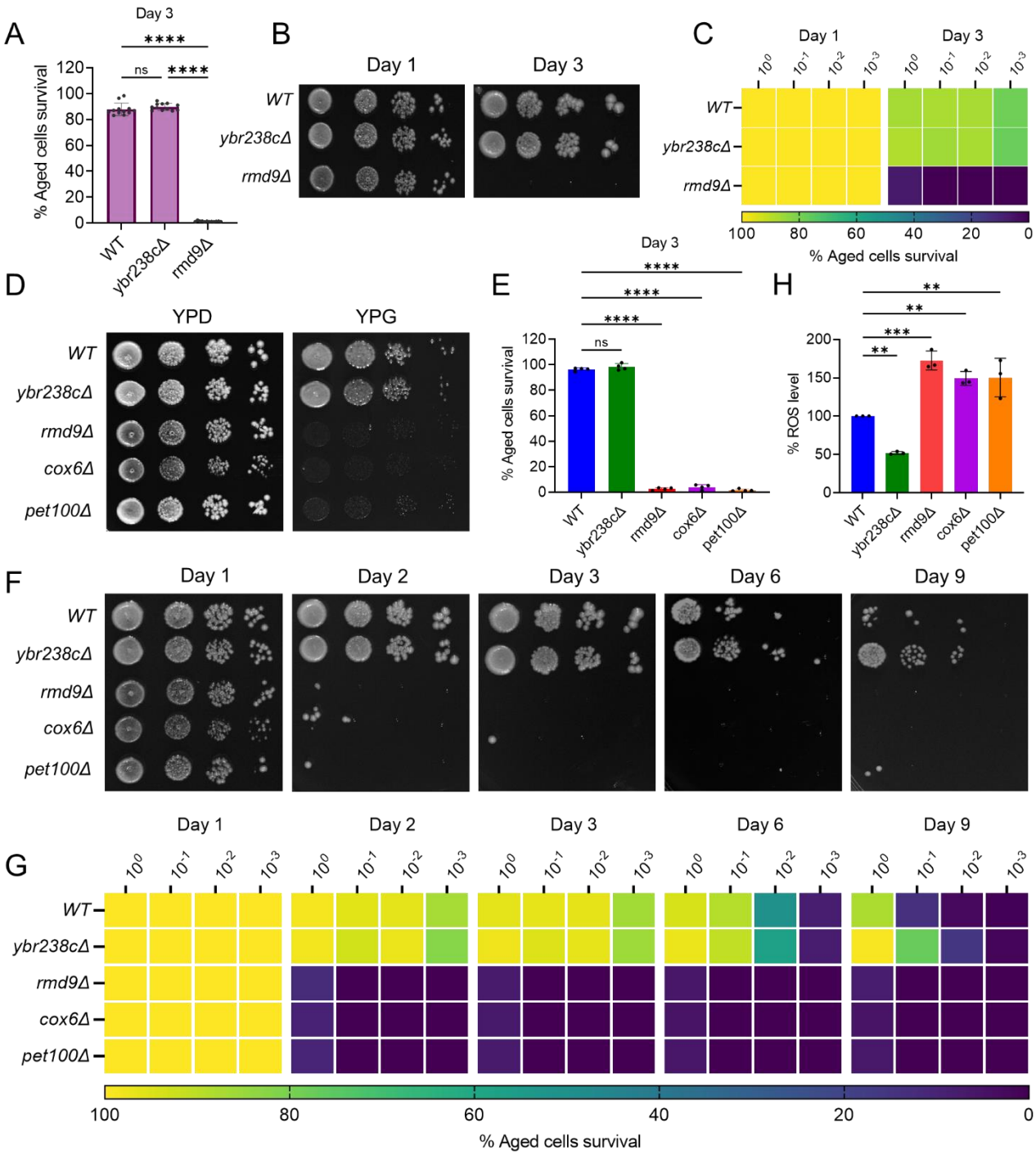
A
Day 3
****
ns
****
% Aged cells survival
120
100
80
60
40
20
0
WT
ybr238cΔ
rmd9Δ
B
Day 1
Day 3
WT
ybr238cΔ
rmd9Δ
C
Day 1
Day 3
WT
ybr238cΔ
rmd9Δ
100
80
60
40
20
0
% Aged cells survival
D
YPD
YPG
WT
ybr238cΔ
rmd9Δ
cox6Δ
pet100Δ
E
Day 3
****
****
****
ns
% Aged cells survival
WT
ybr238cΔ
rmd9Δ
cox6Δ
pet100Δ
H
**
**
***
**
% ROS level
200
150
100
50
0
WT
ybr238cΔ
rmd9Δ
cox6Δ
pet100Δ
F
Day 1
Day 2
Day 3
Day 6
Day 9
WT
ybr238cΔ
rmd9Δ
cox6Δ
pet100Δ
G
Day 1
Day 2
Day 3
Day 6
Day 9
WT
ybr238cΔ
rmd9Δ
cox6Δ
pet100Δ
100
80
60
40
20
0
% Aged cells survival

**Figure S5**

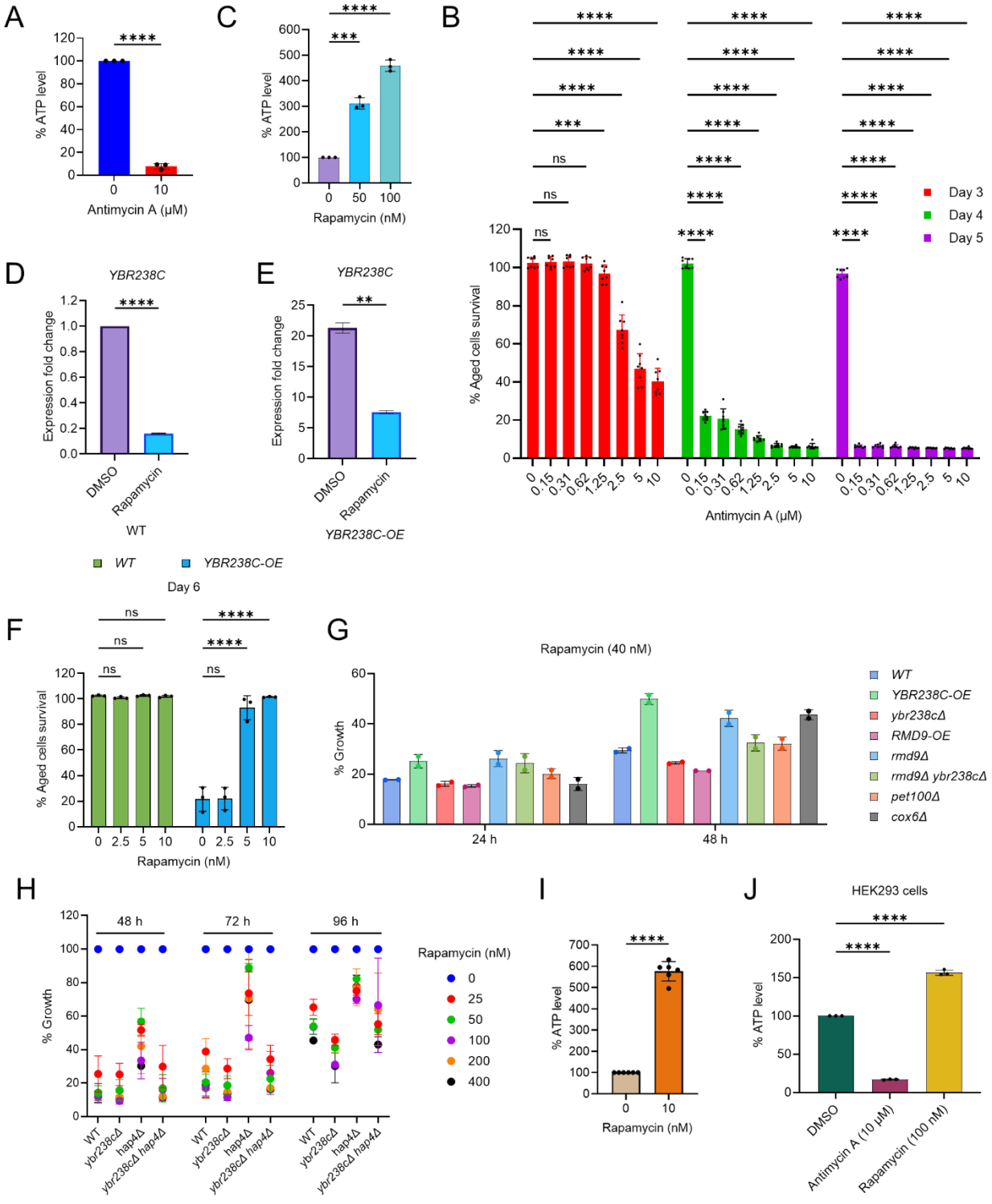
A
% ATP level
Antimycin A (μM)
C
% ATP level
Rapamycin (nM)
B
% Aged cells survival
Antimycin A (μM)
Day 3
Day 4
Day 5
D
YBR238C
Expression fold change
DMSO
Rapamycin
WT
E
YBR238C
Expression fold change
DMSO
Rapamycin
YBR238C-OE
WT
YBR238C-OE
Day 6
F
% Aged cells survival
Rapamycin (nM)
G
Rapamycin (40 nM)
% Growth
24 h
48 h
WT
YBR238C-OE
ybr238cΔ
RMD9-OE
rmd9Δ
rmd9Δ ybr238cΔ
pet100Δ
cox6Δ
H
% Growth
48 h
72 h
96 h
Rapamycin (nM)
WT
ybr238cΔ
hap4Δ
ybr238cΔ hap4Δ
I
% ATP level
Rapamycin (nM)
J
HEK293 cells
% ATP level
DMSO
Antimycin A (10 μM)
Rapamycin (100 nM)

**Figure S6**